Topological fluid mechanics of point vortex motions

Philip Boyland[1], Department of Mathematics, University of Florida, 358 Little Hall, Gainesville, FL 32611-8105

Mark Stremler, Department of Mechanical Engineering, Vanderbilt University, Box 1592, Station B, Nashville, TN 37235

Hassan Aref, Department of Theoretical and Applied Mechanics, University of Illinois, 104 South Wright Street, Urbana, IL 61801

Abstract: Topological techniques are used to study the motions of systems of point vortices in the infinite plane, in singly-periodic arrays, and in doubly-periodic lattices. Restricting to three vortices with zero net circulation, the symmetries are used to reduce each system to a one-degree-of-freedom Hamiltonian. The phase portrait of the reduced system is subdivided into regimes using the separatrix motions, and a braid representing the topology of all vortex motions in each regime is computed. This braid also describes the isotopy class of the advection homeomorphism induced by the vortex motion. The Thurston-Nielsen theory is then used to analyze these isotopy classes, and in certain cases strong implications about the chaotic dynamics of the advection can be drawn. This points to an important mechanism by which the topological kinematics of large-scale, two-dimensional fluid motions generate chaotic advection.

§1 Introduction.

The modeling of incompressible flow at high Reynolds number as a potential flow with embedded vortices has repeatedly proven useful for both analytical and numerical purposes. The subject has inspired numerous reviews, each stressing different aspects of the field. The articles by Aref [Af1], Chorin [C1-3], Leonard [L], Majda [Mj], Moffatt & Tsinober [MfT2], Pullin & Saffman [PS], Saffman & Baker [SB], Saffman [S], Sarpkaya [Srp], Shariff & Leonard [SL], and Zabusky [Z] provide a representative sample. We are concerned here with the further simplification of modeling a two-dimensional flow by a finite collection of point vortices. While this system is admittedly highly idealized, it has found application and, to some extent, experimental verification, starting with von Kármán's analysis in 1912 of the instability of the vortex street wake behind a cylinder and Onsager's 1949 explanation of the emergence of large coherent vortices in two-dimensional flow through an 'inverse cascade' of energy. (See the literature cited for further details.)

In this paper, we study the topology of point vortex motions and the consequences that the topological properties have for the motion of the surrounding fluid. We consider point vortices in the infinite plane, in singly-periodic arrays, and in doubly-periodic lattices. An array of point vortices is useful in modeling shear layers, wakes and jets. The motivation for studying vortex lattices comes from the problem of two-dimensional turbulence, a paradigm of atmospheric and oceanographic flows, and, to a lesser extent, from the study of vortex patterns formed in superfluid Helium.

Kirchhoff recognized that the evolution of N point vortices could be formulated as an N-degree-of-freedom Hamiltonian system ([K]). In many ways, point vortices are the fluid

[1] To whom correspondence should be addressed: `boyland@math.ufl.edu`

mechanical analog of point masses evolving under the mutual interaction of Newtonian gravity. In a Newtonian system, changing the origin of the coordinate system does not influence the motions; this results in conservation of momentum. For point vortices, the analogous constants of motion are called the linear impulses. Unlike the Newtonian case, however, the two components of the linear impulse in vortex systems are only independent if the net circulation is zero. In this case (perhaps the one of most physical interest), the two independent integrals can be used to reduce the Hamiltonian system by two degrees of freedom. Thus for three-vortex systems with zero net circulation, the process of Jacobi-Poincaré reduction yields a single-degree-of-freedom Hamiltonian system (see [Af2], [AS] and [SA]). In such planar systems, the typical orbit is periodic. Since reduction is accomplished by factoring out the translational invariance, trajectories in the reduced system describe the evolution of the shape and orientation of the triangle spanned by the three vortices. As a result, for a periodic motion of the reduced system, the corresponding triangle of vortices resumes its shape and orientation after one period. The vortex motion is thus periodic in the vortex frame, but the triangle could be translated in the lab frame. This translation vector is a dynamic phase of the type that arises when the evolution of a full system is reconstructed from a periodic trajectory of a reduced system.

The further analysis of the phase portrait of the reduced system uses the nonperiodic orbits, namely, the saddle points, separatrices and singularities (see Figures 3.1 and 3.2). The singularities or poles of the reduced Hamiltonian correspond to collisions, or more properly, to the superposition of pairs of vortices, as collisions do not occur when there is zero total circulation. The separatrices naturally divide the phase space into regions (called *regimes* in this paper) in which one would expect the corresponding fluid motions to share certain dynamical characteristics. These characteristics are topological and depend on how the vortices wrap around each other during their evolution. This wrapping is described using Artin's braid group, and we show in §4 that all the vortex motions arising from the same regime are described by the same braid. Thus, the braid description provides a precise language for distinguishing different regimes of vortex dynamics.

In modeling two-dimensional flow with point vortices, the velocity field in the surrounding fluid is generated by the concentrated vorticity at the point vortices. The evolution of passive tracer particles in this velocity field is called advection. For a vortex motion corresponding to a periodic motion of the reduced system, we pass to the vortex frame to eliminate the dynamic phase and so obtain a periodic motion. In this frame, the vortices generate a periodic velocity field, and so we define the advection homeomorphism as the Poincaré map obtained by advecting for one period in this frame. Thus, iterates of the advection homeomorphism describe the dynamics of advection in the vortex frame.

The braid of a regime can be connected to the corresponding advection homeomorphisms using the topological notion of isotopy. A basic theorem says that braids on N strands coordinatize isotopy classes of homeomorphisms on the N-punctured plane ([Bm1]). Thus, because all the motions in a regime have the same braid, they all generate isotopic advection homeomorphisms. This knowledge is then applied using Thurston-Nielsen theory of surface homeomorphisms, which contains a classification theorem for isotopy classes of surface homeomorphisms (a brief introduction to this theory is given in §5). In the case of a pseudoAnosov (pA) isotopy class, the theory gives dynamical behavior that must be present in every homeomorphism in the isotopy class. This information includes a lower bound for such quantities and structures as the growth rate of the number of periodic points as the

period grows, the topological entropy, the growth rate of the length of topologically non-trivial material lines, and the topology of invariant manifold templates. In particular, any homeomorphism in a pA class will be chaotic under any of the usual definitions of the word. In §6 we analyze a zero-circulation, three-vortex-array example with regimes in which the advection homeomorphisms are in pA classes, thus proving that the advection is chaotic in these cases. We also argue that pA classes are common in vortex arrays and lattices.

Note that, in the pA case, detailed information about the induced chaotic advection only requires knowledge of the topology of the point vortex motions. This points to a global, topological mechanism by which large-scale motions cause fluid stretching, mixing and chaotic advection. It is not the concentrated vorticity of the point vortices that is important in this mechanism but rather their role as "stirrers" that displace the fluid, pulling patches of it into the path of other stirrers, which in turn pull it across the paths of other stirrers, etc. The methods of analysis of this paper use the Lagrangian motions of the point vortices to study the Lagrangian motions of fluid particles and thus represent the beginnings of a theory of "topological kinematics." While we focus here on the specific case of three-vortex systems with zero net circulation, it is clear that the same mechanism can act in a much broader class of fluid motions, and we argue in the Conclusion that pA behavior is common in two-dimensional fluid dynamics.

The mathematical tools used here are described in a manner suitable for the application at hand. For a more general and balanced treatment, the reader is urged to consult the references given in each section. The paper [BAS] provides a good complement to this one, applying the same theory to a different fluid flow. The methods used here have also been applied to other systems of physical interest. Any system involving the periodic motions of points in a surface has a natural description using braids. For example, in [Mt] and [Mo], the braid description is used to define constraints for a variational problem. In the Hamiltonian systems they study, the planar positions are configuration variables, and so the conjugate momenta enter into the dynamics. Thus, there is not a homeomorphism of the plane induced by the motion of the points. In other situations where planar point motions do give rise to a natural homeomorphism on the complement of the points, the dynamics of the homeomorphism can be studied using Thurston-Nielsen theory. One such example is when the point motion arises as a periodic orbit in a periodically forced oscillator (see [McT] for a survey). The most general situation starts with an iterated homeomorphism of a surface, focuses on a given collection of periodic orbits, and then examines the isotopy class relative to that set. This situation is fairly well studied (see [Bd] for a survey). Also note that, in [G], pA maps are used to study fast dynamos. In general, topological methods are finding increasing fluid-mechanical applications (see, for example, [AK], [Ri] and [MfT1]).

§2 Equations of motion and Hamiltonians.

We shall be considering the evolution of three types of systems of vortices: finite collections in the infinite plane, singly-periodic arrays, and doubly-periodic lattices. Although all our vortex systems live in the plane, the terminology "planar system" is used here to refer to a finite collection with no periodicity, while "array" and "lattice" refer to singly- and doubly-periodic systems, respectively. Both real and complex notation will be used for points in the plane with $z = x + iy$ in all cases. A *singly-periodic array* of N vortices of period (or width) L is a collection of vortices in the plane with exactly N vortices in each vertical strip of width L and with the property that if there is a vortex at position given by

a complex number z_α, then there is also one at $z_\alpha + nL$ for all integers n. The definition of a vortex lattice requires a pair of linearly independent complex numbers ω_1 and ω_2 (the *half-periods*) that determine the double-periodicity. A *doubly-periodic lattice* of N vortices with lattice structure generated by ω_1 and ω_2 is a collection of point vortices that has exactly N vortices in each fundamental parallelogram determined by $2\omega_1$ and $2\omega_2$, and, if there is a vortex at position z_α, then there is also one at $z_\alpha + n_1 2\omega_1 + n_2 2\omega_2$ for all integers n_1 and n_2. Eventually we shall describe vortex arrays or lattices by singly- or doubly-periodic coordinates, or equivalently, as N vortices on a cylinder or torus. However, initially the arrays or lattices are specified by a collection of N distinguished points. Thus, for example, $(z_1 + L, z_2, z_3)$ represents a different array than (z_1, z_2, z_3). Note also that our definition of lattice requires that it maintain the same periodicity for all time, so a uniformly rotating system is not a lattice in our sense.

We shall assume familiarity with the basics of Hamiltonian systems. Some standard references are [A2], [AM], and [MH].

§**2.1 Equations of motion for the vortex systems.** The α^{th} point vortex has a constant circulation given by the real number Γ_α and a position at time t given by the complex number $z_\alpha(t)$. Using an asterisk to denote the complex conjugate, the evolution of the vortex systems is described by

$$\frac{dz_\alpha^*}{dt} = \frac{1}{2\pi i} \sum_{\beta \neq \alpha} \Gamma_\beta \; \phi_{\mathcal{X}}(z_\alpha - z_\beta) \tag{2.1}$$

for $\alpha = 1, \ \ldots \ , N$. Using $\mathcal{X} = \mathcal{P}$ for the infinite plane, $\mathcal{X} = \mathcal{A}$ for arrays, and $\mathcal{X} = \mathcal{L}$ for lattices, the complex-valued function $\phi_{\mathcal{X}}$ in the various cases is

$$\begin{aligned} \phi_{\mathcal{P}}(z) &= \frac{1}{z} \\ \phi_{\mathcal{A}}(z) &= \frac{\pi}{L} \cot\left(\frac{\pi}{L} z\right) \\ \phi_{\mathcal{L}}(z) &= \zeta(z) + \delta z - \frac{\pi}{\Delta} z^* \end{aligned} \tag{2.2}$$

where in the lattice case, $\zeta(z) = \zeta(z; \omega_1, \omega_2)$ is the Weierstrass zeta function, Δ is the area of a fundamental parallogram, and $\delta = \frac{\pi}{\Delta} - \frac{\zeta(\omega_1)}{\omega_1}$. Note that, in each case, the function ϕ is odd and has the required periodicity; $\phi_{\mathcal{L}}(z + nL) = \phi_{\mathcal{L}}(z)$ and $\phi_{\mathcal{A}}(z + 2n_1\omega_1 + 2n_2\omega_2) = \phi_{\mathcal{A}}(z)$ (the latter identity uses the Legendre relation for the Weierstrass zeta function).

In the presence of the evolving vortex system, a passive particle with position given by $z(t)$ advects according to

$$\frac{dz^*}{dt} = \frac{1}{2\pi i} \sum_{\beta=1}^{n} \Gamma_\beta \; \phi_{\mathcal{X}}(z - z_\beta(t)) \tag{2.3}$$

with the function $\phi_{\mathcal{X}}$ the same as above. One may think of the passive particle as a vortex with zero circulation, and so the advection problem is the analog of the Newtonian $(N+1)$-body problem.

The equations of motion for the plane and array cases are well known. For a derivation of the equations for vortex lattices, see [O] and [SA]. The function ϕ is usually thought of as representing the contribution of a single vortex. It has a simple pole at the position of the vortex and thus contributes a delta function to the curl of the velocity field. Note, however,

that in the lattice case, the function $\phi_{\mathcal{A}}$ is not meromorphic, because for doubly-periodic meromorphic (i.e. elliptic) functions, the residues of the poles in a fundamental parallelogram must sum to zero (equivalently, by Green's Theorem, a doubly-periodic vector field must have zero net curl in each fundamental parallelogram). Thus the concept of a single doubly-periodic vortex or of a lattice (as we have defined it) with non-zero net circulation requires additional consideration. On the other hand, if $\sum \Gamma_\alpha = 0$, as will be assumed below, the right-hand side of (2.3) is an elliptic function of z, and one may speak without contradiction of the effect of the entire lattice on a passive particle.

§**2.2 Hamiltonians.** Since the position of each vortex is specified by a complex number, the state of an N-vortex system is given by an element of $\mathbb{C}^N$. To eliminate singularities, we remove points representing collisions, and so the phase space of an N-vortex system is $\mathbb{C}^N - \Upsilon_{\mathcal{X}}$, where $\Upsilon_{\mathcal{X}}$ is the *collision set* defined in the various cases as

$$\begin{aligned}
\Upsilon_{\mathcal{P}}(z) &= \{(z_1, \ \dots \ , z_N) \in \mathbb{C}^N : z_i = z_j \text{ for some } i \neq j\} \\
\Upsilon_{\mathcal{A}}(z) &= \{(z_1, \ \dots \ , z_N) \in \mathbb{C}^N : z_i = z_j + nL \text{ for some } i \neq j, n \in \mathbb{Z}\} \\
\Upsilon_{\mathcal{L}}(z) &= \{(z_1, \ \dots \ , z_N) \in \mathbb{C}^N : z_i = z_j + 2n\omega_1 + 2m\omega_2 \text{ for some } i \neq j, n, m \in \mathbb{Z}\}.
\end{aligned}$$

The x and y positions of each vortex, x_α and y_α, will be the conjugate variables, and so the Hamiltonian system has N degrees of freedom, but there is no configuration space in the usual sense: the Hamiltonian is defined on a $2N$-dimensional symplectic manifold that is not a cotangent bundle.

In all cases, the real-valued Hamiltonian takes the form

$$H_{\mathcal{X}}(z_1, \ \dots \ , z_N) = -\frac{1}{4\pi} \sum{}' \Gamma_\alpha \, \Gamma_\beta \, \Phi_{\mathcal{X}}(z_\alpha - z_\beta), \tag{2.4}$$

where the sum is over all α and β, and the primed summation symbol indicates that the term $\alpha = \beta$ is excluded. The function $\Phi_{\mathcal{X}}$ (essentially the real part of the antiderivative of $\phi_{\mathcal{X}}$) in the various cases is

$$\begin{aligned}
\Phi_{\mathcal{P}}(z) &= \log(|z|) \\
\Phi_{\mathcal{A}}(z) &= \log\left(\left|\sin\left(\frac{\pi}{L} z\right)\right|\right) \\
\Phi_{\mathcal{L}}(z) &= \log(|\sigma(z)|) + \mathrm{Re}(\frac{\delta z^2}{2}) - \frac{\pi}{2\Delta} z z^*,
\end{aligned} \tag{2.5}$$

where $\sigma(z)$ is the Weierstrass sigma function with half-periods ω_1 and ω_2. The equations of motion (2.1) then have the form

$$\Gamma_\alpha \frac{dz_\alpha^*}{dt} = \frac{\partial H}{\partial y_\alpha} + i \frac{\partial H}{\partial x_\alpha}. \tag{2.6}$$

The presence of the Γ_α indicates that, to put the equations into Hamiltonian form, we need either to change coordinates or to use a slightly nonstandard symplectic form

$$\sum \Gamma_\alpha \, dx_\alpha \wedge dy_\alpha. \tag{2.7}$$

It is clear from equations (2.1) that the complex quantity $J = \sum \Gamma_\alpha z_\alpha$ is a constant of the motion. This integral is associated with the invariance of the Hamiltonian under simultaneous planar translation of all the vortices. Writing $J = Q + iP$ and using the symplectic form (2.7), the Poisson bracket of P and Q is $\{P, Q\} = \sum \Gamma_\alpha$.

The advection equation (2.3) may also be put in Hamiltonian form. Assuming that a motion $\{z_\beta(t)\}$ of the N vortices is given, the time-dependent real-valued Hamiltonian is

$$G_{\mathcal{X}}(z) = -\frac{1}{2\pi} \sum_{\beta=1}^{N} \Gamma_\beta \Phi_{\mathcal{X}}(z - z_\beta(t)). \tag{2.8}$$

In this case we use the standard symplectic form on the plane. The function $G_{\mathcal{X}}$ is more commonly called the *stream function* of the advection problem. The right hand side of (2.8) is the stream function for the velocity field of an unsteady two-dimensional fluid motion generated by the evolving collection of vortices.

One can also combine the systems (2.4) and (2.8) into a single $(N+1)$-degree-of-freedom system, but we do not pursue this point of view here.

§3 Symmetry and reduction.

§3.1 Continuous and discrete symmetries. The Hamiltonian (2.4) is invariant under simultaneous translation of all the vortices,

$$H_{\mathcal{X}}(z_1 + \tau, \ \ldots \ , z_N + \tau) = H(z_1, \ \ldots \ , z_N) \tag{3.1}$$

for $\tau \in \mathbb{C}$. This action of $\mathbb{C}$ (or $\mathbb{R}^2$) is called the *continuous symmetry*. In the planar case, there is also a symmetry associated with rotation of the plane; this symmetry is not shared by arrays and lattices, and so we do not consider it here.

Vortex arrays and lattices have an additional symmetry arising from their spatial periodicity. For arrays,

$$H_{\mathcal{A}}(z_1 + n_1 L, \ \ldots \ , z_N + n_N L) = H_{\mathcal{A}}(z_1, \ \ldots \ , z_N) \tag{3.2}$$

for all collections of integers $n_1, n_2, \ \ldots \ , n_N$. Thus the Hamiltonian is invariant under an action of $\mathbb{Z}^N$. In the lattice case, the Hamiltonian is invariant under a $(\mathbb{Z}^2)^N$ action,

$$H_{\mathcal{L}}(z_1 + n_1 2\omega_1 + m_1 2\omega_2, \ \ldots \ , z_N + n_N 2\omega_1 + m_N 2\omega_2) = H_{\mathcal{L}}(z_1, \ \ldots \ , z_N). \tag{3.3}$$

These will be called the *discrete symmetries*.

§3.2 Reduction. From this point onward, we restrict attention to the case of three vortices, $N = 3$. In addition, the sum of the circulations is assumed to be zero, $\sum \Gamma_\alpha = 0$.

The continuous symmetry expresses the fact that the vortex dynamics is independent of the choice of origin. More precisely, if all the initial positions of the vortices are translated by a fixed amount, then the resulting evolution is also translated by this same fixed amount. This suggests that the relative positions of the vortices $z_1 - z_2, z_2 - z_3$, and $z_1 - z_3$ should be adopted as coordinates. In addition, since $J = \sum \Gamma_\alpha z_\alpha$ is a constant of motion and $\sum \Gamma_\alpha = 0$, we find that once one of these variables is specified, say $Z = z_1 - z_2$, the others are determined as

$$\begin{aligned} z_2 - z_3 &= \frac{-J + \Gamma_1 Z}{\Gamma_3} \\ z_1 - z_3 &= \frac{-J - \Gamma_2 Z}{\Gamma_3}. \end{aligned} \tag{3.4}$$

To compute the equation of motion for Z, substitute (3.4) into the difference of the first two equations of (2.1) yielding

$$\frac{dZ^*}{dt} = \frac{-\Gamma_3}{2\pi i}\left(\phi_{\mathcal{X}}(Z) + \phi_{\mathcal{X}}\left(\frac{-J+\Gamma_1 Z}{\Gamma_3}\right) + \phi_{\mathcal{X}}\left(\frac{J+\Gamma_2 Z}{\Gamma_3}\right)\right). \tag{3.5}$$

This is a one-degree-of-freedom system with Hamiltonian

$$K_{\mathcal{X}}(Z) = \frac{\Gamma_3}{2\pi}\left(\Phi_{\mathcal{X}}(Z) + \frac{\Gamma_3}{\Gamma_1}\Phi_{\mathcal{X}}\left(\frac{-J+\Gamma_1 Z}{\Gamma_3}\right) + \frac{\Gamma_3}{\Gamma_2}\Phi_{\mathcal{X}}\left(\frac{J+\Gamma_2 Z}{\Gamma_3}\right)\right) \tag{3.6}$$

using the standard symplectic form. (Phase portraits in a planar and in an array example are shown in Figures 3.1 and 3.2, respectively). Note that $K_{\mathcal{X}}$ is almost obtained by substituting (3.4) into the Hamiltonian (2.4), but there is a somewhat mysterious factor of $-\Gamma_1\Gamma_2/\Gamma_3$.

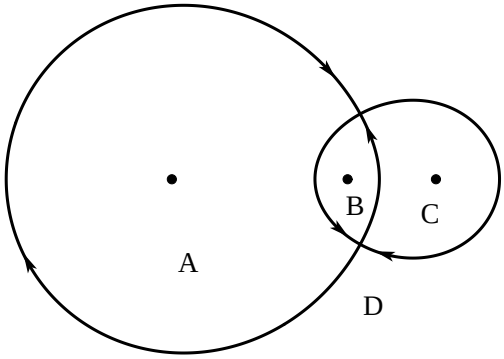

Figure 3.1: Phase portrait of the reduced Hamiltonian system for three vortices in the infinite plane with circulations $1, 1/2$ and $-3/2$. The upper case letters label regimes that are discussed in §4.3.

This process of using continuous symmetries to reduce the number of degrees of freedom of a Hamiltonian system is called *Jacobi-Poincaré* reduction. The mathematical theory of reduction has been much developed in recent years (see, for example, [M], Appendix 5 in [A2], or Chapter V.D in [MH]). Reduction for vortices on the sphere is done in [PM] and in the infinite plane in [AR].

The general process of reduction proceeds by first fixing a value of the integrals connected with continuous symmetries and then identifying elements in this level set that correspond under the restricted symmetry. In the case at hand, these two steps correspond to fixing the value of the integrals P and Q (recall that $J = P + iQ$) and then adopting the coordinate $Z = z_1 - z_2$. Note that each symmetry is used twice, and so reduces the system by two real dimensions, or by one degree of freedom. To reduce a system using multiple symmetries, one must confirm their independence by checking that the Poisson bracket of each pair vanishes. In the case of vortex systems with zero net circulation, $0 = \sum \Gamma_\alpha = \{P, Q\}$, and so the integrals are independent and the system can be reduced by two degrees of freedom, from three to one. The fact that a reduced system is still Hamiltonian is expressed in the Meyer-Marsden-Weinstein Theorem (see [M]). This theorem also gives the correct symplectic form for the reduced system, which in the vortex case is

$$\frac{-\Gamma_1\Gamma_2}{\Gamma_3} dZ^1 \wedge dZ^2$$

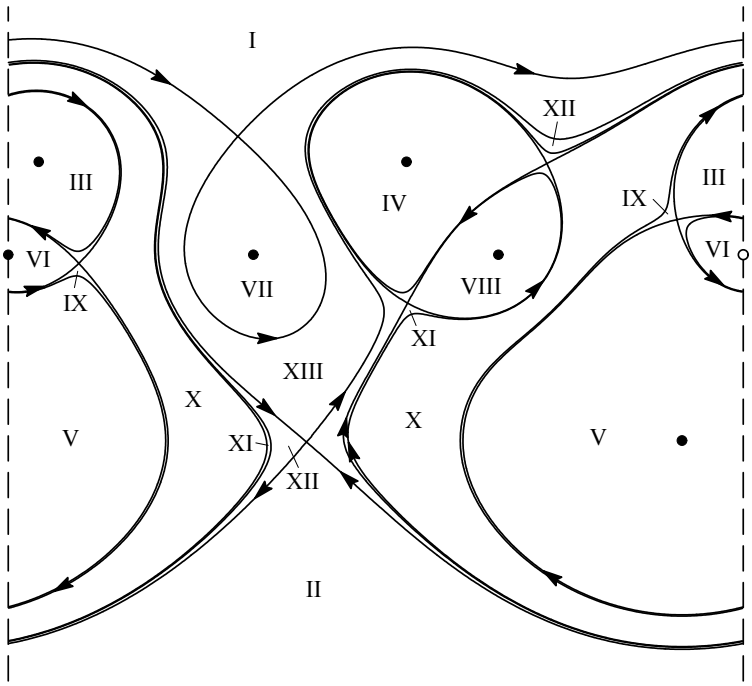

Figure 3.2: Phase portrait of the reduced Hamiltonian system for three vortices in a singly-periodic array with circulations $1, 1/2$ and $-3/2$. The Roman numerals label regimes that are discussed in §4.5.

with $Z = Z_1 + iZ_2$, which explains the factor $-\Gamma_1\Gamma_2/\Gamma_3$ remarked on above.

§**3.3 Discrete symmetries and periodicity of the reduced system.** The discrete symmetries of arrays and lattices give rise to additional considerations in the reduction. For expositional simplicity, we let the spatial periodicities of all arrays and lattices be equal to one, i.e. , $1 = L = 2\omega_1 = 2\omega_2$. We also assume that the circulation $\Gamma_1 = 1$; this can be done with no loss of generality, since by (2.1), a rescaling of all circulations by the same amount only changes the speed (and perhaps the direction) of the vortices but does not change their trajectories.

If $\Gamma_3 = p/q$, a rational number in lowest form, then (3.6) shows that, for arrays, the reduced Hamiltonian $K_{\mathcal{A}}$ is invariant under translations by p. Thus the reduced system has a mod-p symmetry and so is defined on a cylinder of circumference p. In the lattice case, $K_{\mathcal{L}}$ is invariant under translations by p in both directions, and so the system has a mod-p symmetry in both directions and is defined on a torus with circumference p in both directions. Thus, although z_1 and z_2 originally each have a mod-1 symmetry, after reduction, their difference $Z = z_1 - z_2$ has a different periodicity.

To see why this is so, first observe that the discrete symmetries can only be incorporated into the reduction if they preserve the level sets, or equivalently, the value of the integral J. Specifically, if $\sum \Gamma_\alpha z_\alpha = J_0$, then there is no guarantee that $\sum \Gamma_\alpha(z_\alpha + n_\alpha) = J_0$ for an arbitrary triple of integers (n_1, n_2, n_3). However, it is easy to find conditions that insure this, namely, $\sum \Gamma_\alpha n_i = 0$. The set of all such (n_1, n_2, n_3) is a subgroup of $\mathbb{Z}^3$, which we denote $\mathbf{K}$. This subgroup always contains all multiples of $(1, 1, 1)$ and is larger exactly when Γ_3 is rational. Since translation by integer multiples of $(1, 1, 1)$ is contained in the continuous action, we see that the discrete symmetries only come into play when Γ_3 is rational.

The subgroup $\mathbf{K}$ represents the portion of the discrete symmetries that can enter into the reduction. Since an element (n_1, n_2, n_3) in $\mathbf{K}$ acts by translation in each coordinate, the reduced coordinate $Z = z_1 - z_2$ is translated to $Z + (n_1 - n_2)$. But note that for elements of $\mathbf{K}$, $(n_1 - n_2) = \Gamma_3(n_2 - n_3)$ (recall that $\Gamma_1 = 1$). Thus, if $\Gamma_3 = p/q$ is rational (in lowest terms), then since $n_1 - n_2$ is an integer, $n_2 - n_3$ must be divisible by q, and so the action of $\mathbf{K}$ adds p times an integer to the coordinate Z. Since $(2q + p, 2q, q)$ is in $\mathbf{K}$ and it acts by adding exactly p to Z, we see that the induced symmetry on the reduced space is translation by p, and so the reduced Hamiltonian has a mod-p symmetry. Figure 3.2 shows the orbits of the reduced system for a vortex array with $\Gamma_1 = 1, \Gamma_2 = 1/2$, and $\Gamma_3 = -3/2$. The left and right edges of the box can evidently be identified to get a width-3 cylinder.

When Γ_3 is irrational, it induces a quasiperiodicity on the reduced system. This is best understood by viewing reduction from a slightly different angle, using the discrete symmetries first and then the continuous ones. The focus here is on lattices, and we comment on arrays at the end. The nomenclature *n-torus* refers to the topological space $\mathbb{T}^n := (S^1)^n$, i.e. , the n-dimensional manifold that is periodic in all n directions.

By treating each z_α as a doubly-periodic variable, we first view the phase space as a product of three 2-tori minus the collision set. The continuous symmetry of $\mathbb{R}^2$ acts by simultaneous addition on all tori. Identifying points that correspond under this symmetry amounts to adopting periodic coordinates $(U, V) := (z_1 - z_2, z_2 - z_3)$. In geometric language, after we "mod out" by the continuous symmetries, we are left with the product of two 2-tori (minus collisions), which we call $\hat{\mathcal{Y}}$. The Hamiltonian (2.4) descends to

$$\hat{H}(U, V) = -\frac{1}{2\pi}(\Gamma_1\Gamma_2\phi(U) + \Gamma_2\Gamma_3\phi(V) + \Gamma_1\Gamma_3\phi(U + V)).$$

We must be careful, however, because the integral J does not descend to a real-valued function on $\hat{\mathcal{Y}}$. If Γ_3 is an integer, the integral J may be expressed in these coordinates as $\hat{J}(U, V) = U - \Gamma_3 V$ (recall that $\Gamma_1 = 1$) with $\hat{J}$ having values in a 2-torus with width Γ_3 in both directions. If Γ_3 is irrational, no such adaptation may be made. In any case, the important point here is that, since a level set A of J is invariant under the Hamiltonian dynamics, its projection $\hat{A}$ to $\hat{\mathcal{Y}}$ is invariant under the Hamiltonian dynamics induced by $\hat{H}$.

Since the product of two 2-tori is a 4-torus, we may treat $\hat{\mathcal{Y}}$ as a subset of $\mathbb{T}^4$. If Γ_3 is irrational, the projected level set $\hat{A}$ is an immersed 2-plane that winds densely in the 4-torus. The Hamiltonian $\hat{H}$ on $\mathbb{T}^4$ restricted to $\hat{A}$ is the same as the reduced Hamiltonian given in (3.6). Thus this Hamiltonian induces a quasiperiodic system in the sense of [A1]. The function $\hat{H}$ has singularities when $U = 0$, $V = 0$ or $U = -V$, each of which represents a plane in $\mathbb{T}^4$. The intersections of these planes with the densely wrapped plane $\hat{A}$ yield the poles of the reduced Hamiltonian $K_{\mathcal{L}}$. Thus the collection of poles is a quasi-crystal, at least according to one definition of that term ([J], [A1]).

Since the complexification of $\hat{H}$ has simple poles, the poles of the restricted Hamiltonian on any $\hat{A}$ are also simple. Thus it is plausible that the reduced Hamiltonian system can be treated as advection in the presence of fixed vortices with circulations given by the residues of the poles. The precise sense in which this is true is given in [SA] and [AN]. Further, it is shown in [AN] that this collection of fixed vortices is dynamically fixed as well, i.e. , if these vortices are allowed to interact with each other, then they will still be stationary. In other language, the collection of poles of the reduced Hamiltonian gives an equilibrium configuration of the planar N-vortex problem.

A similar analysis can be applied to the array case, but now if Γ_3 is irrational, then the quasi-periodicity of the reduced Hamiltonian $K_{\mathcal{A}}$ is only in the real direction.

§3.4 Reconstruction *Reconstruction* refers to the process of obtaining solutions to the full equations (2.1) for z_1, z_2 and z_3 using the value of J and the solution $Z(t)$ for reduced equation (3.5). This is done by "quadrature." Explicitly, using (3.4) in the differential equation (2.1) for z_1,

$$\frac{dz_1}{dt} = \frac{1}{2\pi i}\left(\Gamma_2\ \phi_{\mathcal{X}}(Z(t)) + \Gamma_3\ \phi_{\mathcal{X}}\left(\frac{-J-\Gamma_2 Z}{\Gamma_3}\right)\right). \tag{3.7}$$

Thus, once an initial position $z_1(0)$ is chosen, $z_1(t)$ may be obtained by integrating (3.7), and then $z_2(t) = z_1(t) - Z(t)$, and (3.4) yields $z_3(t)$.

Note that, if $Z(t)$ is periodic with period P, (3.7) shows that the vortex positions $z_\alpha(t)$ are, in general, not periodic. Rather, there is a constant $b \in \mathbb{C}$ with $z_\alpha(t+P) = z_\alpha(t) + b$ for all t and α. The number b is the *dynamic phase* and it depends only on the periodic orbit $Z(t)$. In the geometric language of reduction, the level set determined by the integrals is a bundle over the reduced space. The geometric phase represents the return map to the fiber (holonomy) in this bundle as one goes around a periodic orbit loop in the reduced space.

To understand the dynamic phase in terms of the geometry of the vortex configuration, recall that the variable $Z = z_1 - z_2$ of the reduced space, with the fixed value of J, determines the shape and orientation of the triangle determined by the vortices. Another variable, which we choose to be z_1, determines its position. The reduced Hamiltonian system has just one degree of freedom, and so the generic bounded orbit is periodic. This means that after some period P, the shape and orientation of the triangle of vortices will be reestablished, but in general, the entire configuration could have translated by some amount, this amount being the dynamic phase b.

§4 Regimes and braids.

§4.1 Braids and braid types. Braids are the standard mathematical tool for describing the topology of periodic motions of points in the plane. This subsection gives a brief introduction to braids from a point of view useful for the applications that follow. For broader perspective and additional information, see [Bm1] or [BL].

A *physical* or *geometric* braid is a collection of non-crossing paths in $\mathbb{R}^3$ that start at some finite collection of points E on the plane where the third coordinate is zero and end at the same set of points (perhaps permuted) on the plane where the third coordinate is one. More formally, a physical braid on n strands is a collection of maps $\mathbf{b} = \{b_1, \ \dots \ , b_n\}$, with each $b_i : [0,1] \to \mathbb{R}^3$ and (1) each b_i has the form $b_i(t) = (a_i(t), t)$ with each a_i continuous, (2) for all $t \in [0,1]$, $b_i(t) \neq b_j(t)$ for $i \neq j$, and (3) the set of initial points is identical to the set of final points $E = \{a_1(0), a_2(0), \ \dots \ , a_n(0)\} = \{a_1(1), a_2(1), \ \dots \ , a_n(1)\}$. The initial and final points of the braid are collectively called the *endpoints*.

A *mathematical braid* on n strands is an element of the braid group B_n. This group is defined as possessing the n generators $\sigma_1, \sigma_2, \ \dots \ , \sigma_n$ with inverses denoted $\bar{\sigma}_1, \bar{\sigma}_2, \ \dots \ , \bar{\sigma}_n$ and the relations $\sigma_i\sigma_j = \sigma_j\sigma_i$ for $|i-j| > 1$ and $\sigma_i\sigma_{i+1}\sigma_i = \sigma_{i+1}\sigma_i\sigma_{i+1}$ for all i ([Bm1]). A *braid word* refers to a sequence of "letters," where each letter is one of the σ_i or its inverse. The inverse of a generator is indicated by an overbar, $\bar{\sigma}_i$. Two braid words are said to be *equivalent* if they represent the same element in the braid group, i.e. , one can be transformed into the other using the relations in the group. The identity element in B_n is denoted e.

The assignment of a mathematical braid to a physical one requires a plane onto which projections are made. The convention here is to let this plane in $\mathbb{R}^3$ be $y = k$ for some large negative k. If we treat the xy plane as the complex numbers, projection of $\mathbf{b}$ onto the chosen plane yields a family of curves $(\mathrm{Re}(a_i(t)), t)$. An *ij-crossing* is a point where $\mathrm{Re}(a_i(t)) = \mathrm{Re}(a_j(t))$ for some t and $i \neq j$. The braid word records which strand is in front at each crossing or, more precisely, which of the $b_i(t)$ is closest to the projection plane.

The braid word corresponding to $\mathbf{b}$ is read off from the picture of the projection. Assume for the moment that all crossings are transverse and take place at distinct times. Starting from the bottom, examine the first crossing. If the i^{th} strand from the left crosses behind the $(i+1)^{\mathrm{st}}$, write down the letter σ_i. If it crosses in front, write $\bar{\sigma}_i$. Now continue upward in the projection, checking each crossing and writing a braid letter. Note that the i^{th} strand at each step refers to the i^{th} strand *from the left* at that level. The physical strand that is i^{th} at one level may become $(i+1)^{\mathrm{st}}$ or $(i-1)^{\mathrm{st}}$ at the next level. It is also worth noting that, contrary to the conventions of [Bm1], the convention here is that letters further to the right in a braid word encode crossings that are *higher* up the braid. We adopt this somewhat nonstandard convention because our physical braids arise from time-parameterized trajectories in the plane, and it is more natural to visualize these in $\mathbb{R}^3$ with time going upwards.

We also need to characterize the physical braids that get assigned to the same mathematical braid. Two physical braids $\mathbf{b}$ and $\mathbf{b}'$ with the same endpoints are *equivalent* if one can be obtained from the other by a deformation that fixes the endpoints and does not cut the strands, i.e. , there is a continuous family of physical braids $\mathbf{b}^s$ for $s \in [0,1]$ with $\mathbf{b}^0 = \mathbf{b}$ and $\mathbf{b}^1 = \mathbf{b}'$. The relations in the braid group are chosen precisely so that two physical braids are equivalent exactly when they are assigned equivalent braid words, i.e. , the same mathematical braid. A theorem of Artin's ([Bm1]) says that any equivalence between physical braids can be described in terms of just the two kinds of deformations described by the relations in the braid group.

Because equivalent physical braids are assigned equivalent braid words, we can eliminate the assumption that we had to make to assign a mathematical braid to a physical one. If $\mathbf{b}$ does not have transverse and time-distinct crossings, then deform it to another braid $\mathbf{b}'$ that does and compute a mathematical braid for $\mathbf{b}'$. Since any other "good" deformation will be assigned a braid word equivalent to that of $\mathbf{b}'$, this braid word may be used unambiguously for $\mathbf{b}$.

Thus far, we have restricted attention to the equivalence of physical braids with the same endpoints. Since the braids here arise from vortex motions with a variety of initial positions, we need to extend the notion of equivalence. Informally, two braids with perhaps different endpoints are equivalent if one can be transformed into the other via a plane transformation applied on each horizontal plane followed by a deformation with fixed endpoints. More formally, two physical n-braids $\mathbf{b}$ and $\mathbf{b}'$ are *equivalent* if there is a homeomorphism $h : \mathbb{R}^2 \to \mathbb{R}^2$ with $h(a_i(0)) = a_i'(0)$ for all i and the physical braid $\{(h(a_i(t)), t)\}$ is equivalent with fixed endpoints to $\mathbf{b}'$. A simple argument shows that physical braids that are equivalent in this sense are assigned conjugate elements of the braid group, i.e. , the words satisfy $w' = gwg^{-1}$, where g is an element of the braid group that represents the homeomorphism h. Note that a change of the projection plane may be accomplished by an affine map of the plane, and so the mathematical braid obtained using the new projection plane is conjugate to the original.

Since the goal here is to use braids to analyse the topology of vortex motions, topologically equivalent physical braids and physical braids viewed by different observers must be

assigned the same mathematical object. The remarks of the last paragraph make it clear that this object cannot be just a mathematical braid, but rather must be a conjugacy class in the braid group, i.e. , the collection of all elements conjugate to a given one (and thus conjugate to each other). These conjugacy classes were called *braid types* in a related context and that terminology is adopted here (cf. [Bd]). For simplicity of exposition in the sequel, we will often speak informally of the *braid* associated to a physical braid, but a more careful terminology would be *braid type*.

§**4.2 Three vortices in the plane.** In assigning braids to the motion of three point vortices in the infinite plane, we continue to focus on the case of zero net circulation, $\sum \Gamma_\alpha = 0$. As in §3, we fix a value of the integral $J_0 = Q_0 + iP_0$, perform the reduction, and obtain the Hamiltonian (3.6) on a copy of the plane R with complex coordinate Z.

Pick an initial condition Z_0 in R that is contained in a periodic orbit $Z(t) := Z(t; Z_0)$ with period P. Using (3.4), the motion $Z(t)$ determines the evolution of the differences in the positions of the three vortices. Thus $Z(t)$ can be used to compute the motion in the frame of one of the vortices. In the z_2-frame, this motion is described by

$$\begin{aligned} Z_1(t) &:= z_1(t) - z_2(t) = Z(t) \\ Z_2(t) &:= z_2(t) - z_2(t) \equiv 0 \\ Z_3(t) &:= z_3(t) - z_2(t) = \frac{J_0 - \Gamma_1 Z(t)}{\Gamma_3}. \end{aligned} \tag{4.1}$$

Thus all the Z_α's are periodic with period P. Note that $z_\alpha \neq z_\beta$ for $\alpha \neq \beta$ (i.e. , the absence of collisions between vortices) is equivalent to $Z_\alpha \neq Z_\beta$ for $\alpha \neq \beta$. Again using (3.4), this happens as long as $Z(t)$ avoids the points $p_1 := J_0/\Gamma_1, p_2 := -J_0/\Gamma_2$, and $p_3 := 0$. The points p_α are the *poles* of the Hamiltonian $K_{\mathcal{P}}$ from (3.6).

The vortex motions generate a physical braid by embedding the motion in $\mathbb{R}^3$ and treating the vertical direction as time. This is done by defining

$$\hat{Z}_\alpha = (Z_\alpha(t), t), \tag{4.2}$$

for $\alpha = 1, 2, 3$. Each path $\hat{Z}_\alpha$ then connects a point on the plane $t = 0$ to the same point on the plane $t = P$, and further, since $Z(t)$ does not pass through any of the poles, the paths do not intersect. Thus, the paths yield a physical braid on three strands, which may be assigned an element of B_3 as in the previous subsection.

This assignment is most easily accomplished by taking a more topological point of view. If we define $R^o = R - \{p_1, p_2, p_3\}$, then the periodic orbit $Z(t)$ in R represents a closed curve (or loop) in R^o. The procedure used to construct a physical braid from $Z(t)$ can equally well be used to assign one to any loop in R^o. If γ is a loop in R^o, i.e. , $\gamma : [0, 1] \to R^o$ with $\gamma(0) = \gamma(1)$, let Z_1, Z_2, Z_3 represent the three paths given by (4.1) using $Z(t) = \gamma(t)$. The physical braid corresponding to γ is then generated by (4.2).

The computation of the mathematical braid corresponding to this physical braid just requires a knowledge of the crossing of its strands. Since our view is from the negative imaginary axis, the positions of the Z_α from left to right are determined by their real parts. Strands cross exactly when this order changes. This can only happen when $\mathrm{Re}(Z_\alpha(t)) = \mathrm{Re}(Z_{\alpha'}(t))$, or equivalently, when $\mathrm{Re}(Z(t)) = \mathrm{Re}(p_\beta)$, where β is the index different from α and α'. Thus the vertical lines through the poles divide R^o into vertical strips in which the order of the Z_α from left to right is constant. These vertical lines will be called *crossing lines*.

To specify the generator corresponding to the crossing of one of these lines, it is also necessary to know which strand is in front. This information is determined by the sign of $\mathrm{Im}(Z(t_c)) - \mathrm{Im}(p_\beta)$ when t_c is the crossing time and $Z(t_c)$ lies on the crossing line $\mathrm{Re}(Z) = \mathrm{Re}(p_\beta)$. This sign can only change on a crossing line when $\mathrm{Im}(Z(t_c)) - \mathrm{Im}(p_\beta) = 0$, i.e. , at the pole. Thus all the crossings on the same side of the pole correspond to the same strand being in front. We will call a component of a crossing line minus its pole a *generator arc*. The final piece of information needed to specify the generator describing a crossing is the direction in which γ traverses the generator arc. In summary, then, any two crossings of a generator arc in the same direction contribute the same generator to the braid. Thus, to compute braids of loops or actual vortex motions, it suffices to compute the generators corresponding to each generator arc. A sample computation is given in the next subsection.

There are two issues that need to be clarified before moving on to the example. First, unlike a mathematical loop, there is no distinguished starting point for a periodic motion of the vortices. However, changing the initial point on $Z(t)$ only cyclically permutes the generators in the braid word that represents the motion. This corresponds to conjugating the word in the braid group, and this ambiguity has already been resolved using the braid type. The second issue is that the usual generators of the braid group B_3 only keep track of which adjacent strands are crossing and not the numbering of the stands. Thus, in assigning a braid generator to a crossing, we have lost track of which vortex has crossed which; our braid word only encodes the topological type of the interaction, and not whether, say, vortices 2 and 3 are the pair that are circling each other. However, this information can be recovered easily by knowing the relative positions of the vortices at the starting point of the braid and following the strands.

§**4.3 A planar example.** Figure 4.1 shows the crossing lines for the planar case of Figure 3.1. The pair of numbers at the top of the crossing line indicates which pair of vortices is crossing. Each generator arc has a number j and an arrow; crossing the arc in the direction of the arrow contributes the positive generator σ_j to the braid word. Crossing in the opposite direction contributes the inverse of this generator, $\bar{\sigma}_j$. The braid word corresponding to a loop $\gamma(t)$ can be computed by writing, in order, the generators corresponding to $\gamma(t)$'s sequential crossings of generator arcs.

As an example, let us compute the braid word corresponding to periodic orbit $Z'(t)$ indicated in Figure 4.1 which is in the region that was labeled D in Figure 3.1. Begin tracking the motion at the starting point labeled $Z'(t_0)$ in the upper left-hand corner. At this point, the vortices from left to right are $1, 3, 2$. The first generator arc crossed is above the pole p_2, and it contributes a σ_1 to the braid word. Moving across horizontally, the next generator arc contributes a σ_2, and so on. When we return to the initial point, the entire braid word $\sigma_1\sigma_2\sigma_1\sigma_1\sigma_2\sigma_1$ has been read off. This braid is shown in Figure 4.2c, with the strands labeled below. By examining the braid we see that this motion corresponds to the vortices rotating clockwise around each other and that this motion is topologically the same as all the vortices rotating once around a circle clockwise. This becomes especially clear after using the braid relation and rewriting the braid as $(\sigma_1\sigma_2)^3$.

Figure 4.2a shows the planar trajectories of three vortices corresponding to the periodic orbit $Z'(t)$. Recall from §3.2 that there are many vortex motions corresponding to a given periodic orbit in R, but all these motions differ by a uniform translation, so it suffices to pick an initial position of one of the vortices, say $z_2(0) = 0$. Figure 4.2b shows the physical

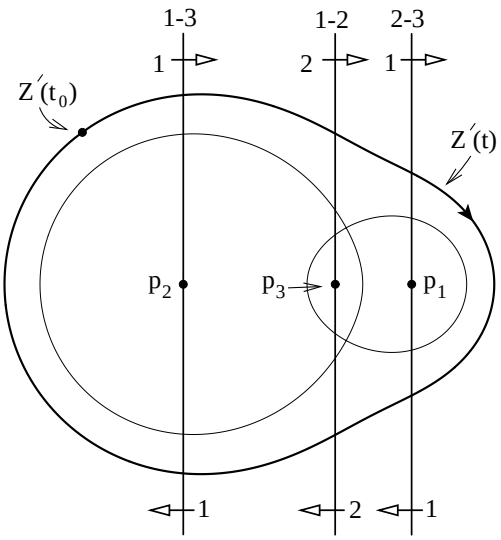

Figure 4.1: The crossing lines and generator arcs for the system shown in Figure 3.1.

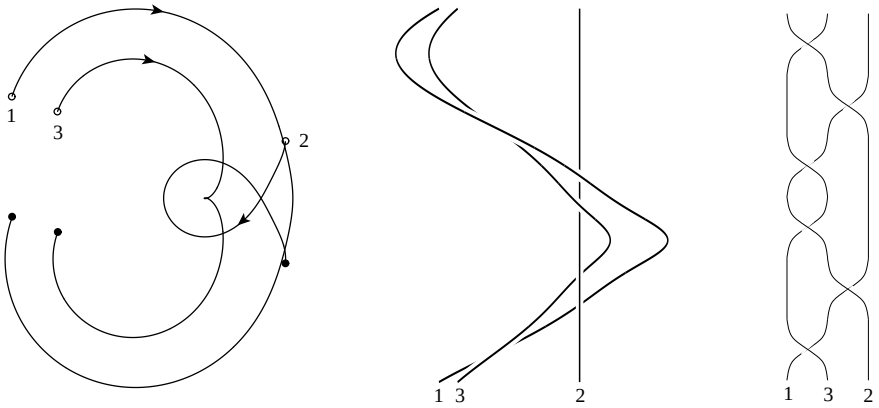

Figure 4.2: Vortex motions from regime D of Figure 3.1. (a) Trajectories of the three vortices in the plane. (b) Physical braid of this motion in the frame of the second vortex. (c) Mathematical braid of the motion.

braid corresponding to the vortex motion in the frame of the second vortex as given by (4.1) and (4.2).

The other regions A, B, and C each contain a pole. The braid that describes each of these regimes is the square of a generator and corresponds to a pair of vortices rotating about each other once per period. There is no linking with the third vortex. The pair of vortices that is involved in the rotation depends on the pole in question, and the direction of the rotation (i.e. , whether the braid is σ_i^2 or $\bar{\sigma}_i^2$) depends on the signs of the circulations of the interacting vortices.

Recall that a *separatrix* is an orbit that connects two saddle points. Define a *regime* as a connected component of $R - \{\text{poles and separatrices}\}$. It is clear from Figure 4.1 that every periodic orbit in the same regime yields the same sequence of crossings of generator arcs, and, thus, the same braid word. Therefore, all the motions within a regime have the

same topological type of motion. More generally, any pair of loops that can be continuously deformed into each other (i.e. , are homotopic) in R^o are assigned the same braid; homotopic loops may cross different generator arcs, but any extra crossings consist of a collection of crossings and then reverse crossings of the same generator arcs. From another point of view, deforming the loop corresponds to deforming the physical braid. The corresponding mathematical braid only changes when a pair of strands goes though each other. This can only happen when the loop passes through a pole, which is not allowed, as all our loop deformations are in the complement of the poles.

This situation is somewhat analogous to the residue theorem, in which a deformation of a closed path in the complement of the poles does not change the value of the integral. However, the situation here is more restrictive: *homologous* loops yield the same integral but only *homotopic* loops give the same braid. In algebraic language, after fixing a base point for loops, the process described here gives a homomorphism from the fundamental group of the punctured plane, $\pi_1(R^o)$, to the braid group on three strands, B_3.

Although all periodic orbits in the same regime have the same braid, it is important to note that the period P and dynamic phase b of the periodic orbits in a single regime can vary greatly. The period goes to zero near a pole and approaches infinity as orbits near a separatrix. Thus, the time scale of the actual vortex motions in the same regimes can be very different. In addition, variations in the dynamic phase can make a significant difference in the motion as observed in the lab frame.

§**4.4 Three-vortex arrays.** This subsection develops the tools needed to assign a braid to the periodic motion of three vortices in a singly-periodic array. We continue to restrict attention to the case of zero net circulation $\sum \Gamma_\alpha = 0$. Fix a value of the integral $J_0 = Q_0 + iP_0$ and perform the reduction as in §3. The result is a Hamiltonian system given by (3.6) on a copy of the plane R with complex coordinate Z. If Γ_3 is the rational number p/q (in lowest terms), then the system on R has a mod-p symmetry in the real part.

By treating each vortex position z_α as a singly-periodic variable, the vortex motion can be viewed as taking place on a cylinder $S^1 \times \mathbb{R}$ (the circle S^1 here has perimeter 1 since we continue to restrict to the case $L = 1$). Equivalently, in the language of §3, we factor out all the motions by the discrete symmetry. Again we eliminate the dynamic phase by passing to the frame of the second vortex, thus making the motion periodic. Accordingly, let

$$\begin{aligned} c_1(t) &:= z_1(t) - z_2(t) = Z(t) \\ c_2(t) &:= z_2(t) - z_2(t) \equiv 0 \\ c_3(t) &:= z_3(t) - z_2(t) = \frac{J_0 - \Gamma_1 Z(t)}{\Gamma_3}, \end{aligned} \tag{4.3}$$

in which, properly speaking, the subtraction is done in the Lie group $S^1 \times \mathbb{R}$. The triple $(c_1(t), c_2(t), c_3(t))$ is called the *cylinder motion* of the vortices.

A braid describes the motion of a set of points in the plane. To translate the cylinder motion to the plane, recall that the cylinder is topologically equivalent to the punctured complex plane $\mathbb{C} - \{0\}$. This topological equivalence is realized by the conformal map $T(z) = \exp(2\pi i z)$. Under this conformal map, a path around the cylinder is transformed to a path around the origin in the complex plane. To capture this type of motion in the braid description, we add the constant path at 0 as the last coordinate of the motion in the plane.

Thus the *plane motion* of the vortices is given by

$$\begin{aligned} s_1(t) &:= T(c_1(t)) = \exp(2\pi i Z(t)) \\ s_2(t) &:= T(c_2(t)) \equiv 1 \\ s_3(t) &:= T(c_2(t)) = \exp\left(2\pi i \frac{J_0 - \Gamma_1 Z(t)}{\Gamma_3}\right) \\ s_4(t) &\equiv 0. \end{aligned} \tag{4.4}$$

Using the same technique as in the previous subsection, we associate a braid (now on four strands) to the plane motion of a three-vortex array. Again we visualize the plane motion in three dimensions using (4.2) with time going upward and view the resulting strands from the negative imaginary axis. The *crossing curves* in R describe the positions of an orbit $Z(t)$ at which s_α and s_β cross; this happens when their real parts are equal. To express this in equation form, define four functions on R by $\psi_1(Z) = T(Z), \psi_2(Z) = 1, \psi_3(Z) = T((J_0 - \Gamma_1 Z)/\Gamma_3)$, and $\psi_4(Z) = 0$. Then $s_\alpha(t) = \psi_\alpha(Z(t)) = T(c_\alpha(t))$, and the (α, β) crossing lines are defined by the equation $\mathrm{Re}(\psi_\alpha(Z)) = \mathrm{Re}(\psi_\beta(Z))$. In contrast to the planar case, these equations no longer yield just straight lines, and, thus, we change the terminology to crossing *curves*.

The strand that is in front at a crossing is determined by the sign of $\mathrm{Im}(s_\alpha(t_c)) - \mathrm{Im}(s_\beta(t_c))$ when $\gamma(t_c)$ is on the corresponding crossing curve. This sign changes on the crossing curve exactly when $s_\alpha = s_\beta$, which corresponds to the poles of the Hamiltonian (3.6). Note that it is no longer the case that every crossing curve contains a pole. This means that crossing anywhere on the curve yields the same generator of the braid word, i.e. , the entire curve is a single generator arc.

§**4.5 An array example.** We now perform the calculations described in §4.4 on the array case shown in Figure 3.2. See [SA] for a details on this and other array examples. The crossing curves corresponding to s_1 and s_3 are defined by $\mathrm{Re}(\psi_1(Z)) = \mathrm{Re}(\psi_3(Z))$, which, writing $Z = x + iy$, is

$$\exp(-2\pi y)\cos(2\pi x) = \exp\left(-2\pi(\tfrac{2}{3}y - \tfrac{1}{4})\right)\cos\left(2\pi(\tfrac{2}{3}x - \tfrac{1}{12})\right).$$

Both cosine terms can vanish yielding the two vertical lines $x = 5/4$ and $x = 11/4$. Otherwise we may solve for

$$y = \frac{3}{2\pi}\left(\log\left(\frac{\cos 2\pi x}{\cos 2\pi(\frac{2}{3}x - \frac{1}{12})}\right) - \frac{\pi}{2}\right),$$

which is defined only on the (mod-3) intervals $(-3/4, 1/4), (1/2, 3/4)$, and $(7/4, 2)$. Thus there are five distinct $(1,3)$-crossing curves. The computations for the other pairs are similar, and the various crossing curves are shown in Figure 4.3a. The numbers that are separated by a hyphen indicate which pair of s_α's is crossing. Note that, since the vertical lines $x = 5/4$ and $x = 11/4$ correspond to $0 = \mathrm{Re}(s_1) = \mathrm{Re}(s_3)$, and we are considering 0 as the position of s_4, these vertical lines correspond to a triple crossing.

The poles are the points 0, 1, and 2, corresponding respectively to $s_1 = s_2$; the points $\frac{1}{8} + \frac{3}{8}i$ and $\frac{13}{8} + \frac{3}{8}i$ corresponding to $s_2 = s_3$; and the point $-\frac{1}{4} - \frac{3}{4}i$ corresponding to $s_1 = s_3$. Figure 4.3b shows the results of computing the generator arcs, with labels that use the same conventions as in Figure 4.1.

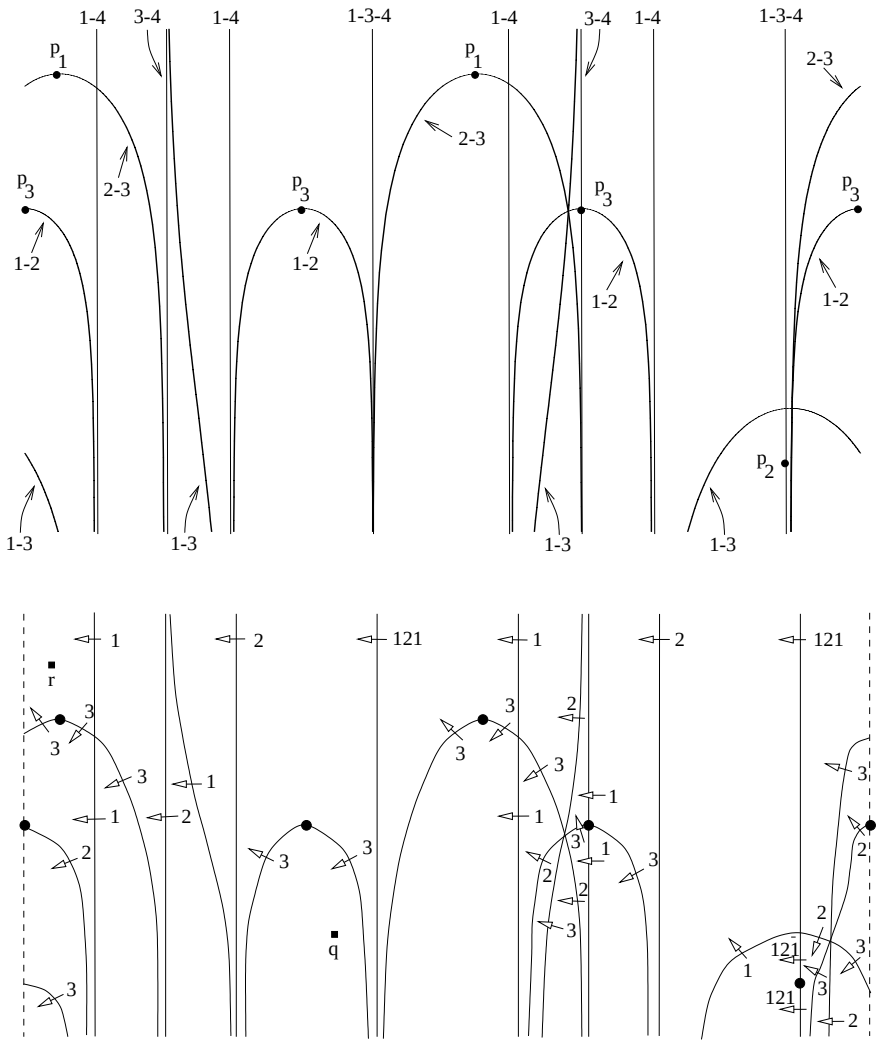

Figure 4.3: (a) Crossing curves and (b) generator arcs for the system in Figure 3.2 (the picture in (b) has been distorted for increased clarity). The points labeled q and r correspond to initial points of trajectories as explained in the text.

It is important to note that the details of Figure 4.3 are not intrinsic to the vortex motions. Changing the projection plane used to compute the braids would change all the crossing curves. However, the braid that is computed for a loop is intrinsic up to conjugacy. In algebraic language, after fixing a base point, the equations (4.4) (using $Z(t)$ to represent a general loop) may be used to define a homomorphism of $\pi_1(R - \{\text{poles}\}) \to B_4$. This homomorphism is not intrinsic, but it is intrinsic up to conjugacy in B_4.

Now define a regime as in the planar case, i.e. , as a connected component of $R - \{\text{poles and separatrices}\}$. Each periodic orbit in a regime gives rise to the same mathematical braid; these are listed in the second column of Table 4.1. Note that the relations in the braid group have been used to simplify many of the braid words. The braids for regimes I and IX through XIII were computed using closed trajectories with initial position near the point labeled r in Figure 4.3b. The initial position used for regime II was near the point labeled q.

Regime	Braid	TN type	Expansion Constant
I	$(\bar{\sigma}_1\bar{\sigma}_2)^3\bar{\sigma}_1^2(\bar{\sigma}_2\bar{\sigma}_1)^3$	reducible, all f.o.	
II	$\sigma_3\sigma_2(\sigma_1\sigma_2\sigma_3)^2\sigma_2\sigma_3\sigma_1\sigma_2\sigma_1(\sigma_1\sigma_2\sigma_3)^2\sigma_2\sigma_1\sigma_3\sigma_1\sigma_2\sigma_1\sigma_3$	reducible, all f.o.	
III	σ_3^2	reducible, all f.o.	
IV	σ_3^2	reducible, all f.o.	
V	σ_1^2	reducible, all f.o.	
VI	$\bar{\sigma}_2^2$	reducible, all f.o.	
VII	σ_3^2	reducible, all f.o.	
VIII	$\bar{\sigma}_3^2$	reducible, all f.o.	
IX	$\sigma_3^2\sigma_2^2$	reducible, all f.o.	
X	$(\sigma_3\sigma_2)^3$	reducible, all f.o.	
XI	$(\sigma_3\sigma_2)^2\sigma_3\sigma_1\sigma_2\sigma_1^2\sigma_2\sigma_1\sigma_2\sigma_3\sigma_1\sigma_3(\bar{\sigma}_1\bar{\sigma}_2)^3\bar{\sigma}_1$	pA	13.93
XII	$(\sigma_3\sigma_2)^2\sigma_3\sigma_1\sigma_2\sigma_1^2(\sigma_2\sigma_3\sigma_1\sigma_3)^2(\bar{\sigma}_1\bar{\sigma}_2)^3\bar{\sigma}_1$	reducible, one pA	13.93
XIII	$(\bar{\sigma}_1\bar{\sigma}_2)^2\bar{\sigma}_3^2(\bar{\sigma}_2\bar{\sigma}_1)^5$	pA	9.90

Table 4.1: The mathematical braids and Thurston-Nielsen type of the regimes for the system shown in Figure 3.2. The expansion constants for pseudo-Anosov (pA) components are given. In the finite order (f.o.) case, these constants are 1. This means that there is no intrinsic topological expansion in that case.

As a sample, we compute the mathematical braids corresponding to regimes I and XIII. The closed orbits in regime I travel across the top of the reduced plane from left to right. To compute the braid, we choose the point labeled r in Figure 4.3b as the initial point. Moving to the right from this point we first traverse a vertical line on which there is an arrow labeled 1. This indicates that the motion of the trajectory has resulted in a crossing of the two left most strands in the physical braid representing the vortices. Further, since the trajectory's motion is opposite to that of the arrow, the strands are crossing with the left one in front of the right one. Thus the traversal of the first crossing curve contributes the letter $\bar{\sigma}_1$ to the braid word of the trajectory. Continuing to the right, the trajectory traverses a crossing curve on which there is an arrow labeled 2, and the arrow points in the direction opposite to the traverse. Thus, this motion contributes a $\bar{\sigma}_2$ to the braid word of the trajectory. Continuing across the top of Figure 4.3b, we add braid letters $\bar{\sigma}_1$, then $\bar{\sigma}_2$, etc. After encountering the right edge of the phase plane, the identification with the left edge allows a return to the initial point. The entire braid word for this regime is thus

$$\bar{\sigma}_1\bar{\sigma}_2\bar{\sigma}_1\bar{\sigma}_2\bar{\sigma}_1\bar{\sigma}_2\bar{\sigma}_1\bar{\sigma}_1\bar{\sigma}_2\bar{\sigma}_1\bar{\sigma}_2\bar{\sigma}_1\bar{\sigma}_2\bar{\sigma}_1 = (\bar{\sigma}_1\bar{\sigma}_2)^3\bar{\sigma}_1^2(\bar{\sigma}_2\bar{\sigma}_1)^3.$$

The closed trajectories for regime XIII have a motion similar to those of regime I with the crucial topological difference that they pass below the pole p_3, which is located at $1+0i$. This implies that, in the complement of the poles, the closed loops corresponding to regimes I and XIII are *not* homotopic. Beginning a closed trajectory representing regime XIII near the point r, the braid word starts with $\bar{\sigma}_1\bar{\sigma}_2\bar{\sigma}_1\bar{\sigma}_2$ like that of regime I, but since the loops for regime XIII pass below the point p_3, their braid words have a $\bar{\sigma}_3\bar{\sigma}_3$ next, and then continue with the same letters as regime I. The entire braid word for regime XIII is thus

$$\bar{\sigma}_1\bar{\sigma}_2\bar{\sigma}_1\bar{\sigma}_2\bar{\sigma}_3\bar{\sigma}_3\bar{\sigma}_1\bar{\sigma}_2\bar{\sigma}_1\bar{\sigma}_1\bar{\sigma}_2\bar{\sigma}_1\bar{\sigma}_2\bar{\sigma}_1\bar{\sigma}_2\bar{\sigma}_1.$$

Note that the braid relation $\bar{\sigma}_1\bar{\sigma}_2\bar{\sigma}_1 = \bar{\sigma}_2\bar{\sigma}_1\bar{\sigma}_2$ used on the triple of letters right after the $\bar{\sigma}_3\bar{\sigma}_3$ allows us to reduce the word to $(\bar{\sigma}_1\bar{\sigma}_2)^2\bar{\sigma}_3^2(\bar{\sigma}_2\bar{\sigma}_1)^5$, as given in Table 4.1.

We now briefly describe some of the motions. In these descriptions we will use the word "vortex" to refer to the trajectories of the planar motions, s_1, s_2, s_3, and s_4. Properly speaking, s_1, s_2, and s_3 are the transformed positions of the vortices, and s_4 is not a vortex at all, but rather it keeps track of the position of the origin.

Before interpreting the braid, it is useful to recall the various transformations that have been used. The motion in the singly periodic plane is really of infinite families of vortices. These families are treated as three individual vortices on a cylinder, and then this motion is transformed to the punctured plane. Thus, a strand in the braid rotating about the strand representing vortex 4 (i.e. , the origin) describes motion around the cylinder, which in turn is a horizontal translation by one period of the corresponding family of vortices in the singly-periodic plane. In addition, the braid is obtained using the frame of the second vortex, so, in particular, vortex 2 will never rotate around the origin, and thus the strands corresponding to vortex 2 and 4 will always be parallel.

The regimes with the simplest braids are those that contain a pole, III through VIII. The vortex motions are topologically the same as regions A, B, and C in the plane case: a pair of vortices are circling each other and the other vortex is uninvolved. There is no rotation around the origin; thus, there is no net rotation around the cylinder.

The vortex motions corresponding to regime X also have no net motion around the cylinder (see Figure 6.1a). This is indicated by the fact that none of the other strands link with the far left one, which represents the origin of $\mathbb{C}$. Examining the right-hand sub-braid on 3 strands, one sees that every vortex rotates about every other one once in the clockwise direction. The net motion is the same as that in the planar region D, and it amounts to one full rotation of the vortices as a group. The motions in regime IX are similar, but the sub-braid is slightly different: vortices 2 and 3 rotate about each other clockwise, and then vortices 1 and 3 do likewise, but vortices 1 and 2 do not link.

The regimes with the next simplest braids are I and II. The mathematical braid for I is shown in Figure 4.4d. Vortex 1 rotates three times around the origin counter-clockwise and vortex 3 rotates twice, also counter-clockwise. This rotation takes place "inside" the fixed vortex 2. In the singly periodic plane, this corresponds to the vortex 1 family translating three strips to the right and the vortex 3 family two strips; this translation takes place below the position of vortex 2. This motion is shown in Figure 4.4a, with one vortex from each singly periodic family pictured. Figure 4.4b shows the motion in the frame of the second vortex after it has been transformed to the plane. The physical braid of this motion constructed using (4.4) and (4.2) is shown in Figure 4.4c. The motion in regime II is similar, but now the rotation is clockwise, and goes around vortex 2, which simply means that in the singly-periodic plane the translations of vortex 1 and 3 are above the position of vortex 2.

The motion in regimes XI, XII, and XIII is sufficiently complicated that the braid itself is the best description of the motion. One feature of interest in regime XII (see Figure 6.1b) is that the vortex pairs 1 and 3 have the same motion with respect to the other two strands while they rotate about each other three times. This kind of hierarchy of motion is described precisely by the notion of reducibility introduced in §5.

§**4.6 Three-vortex lattices.** The method of analysis of this section can also be applied to vortex lattices. When $\Gamma_3 = p/q$ is rational, the reduced Hamiltonian system (3.6) can

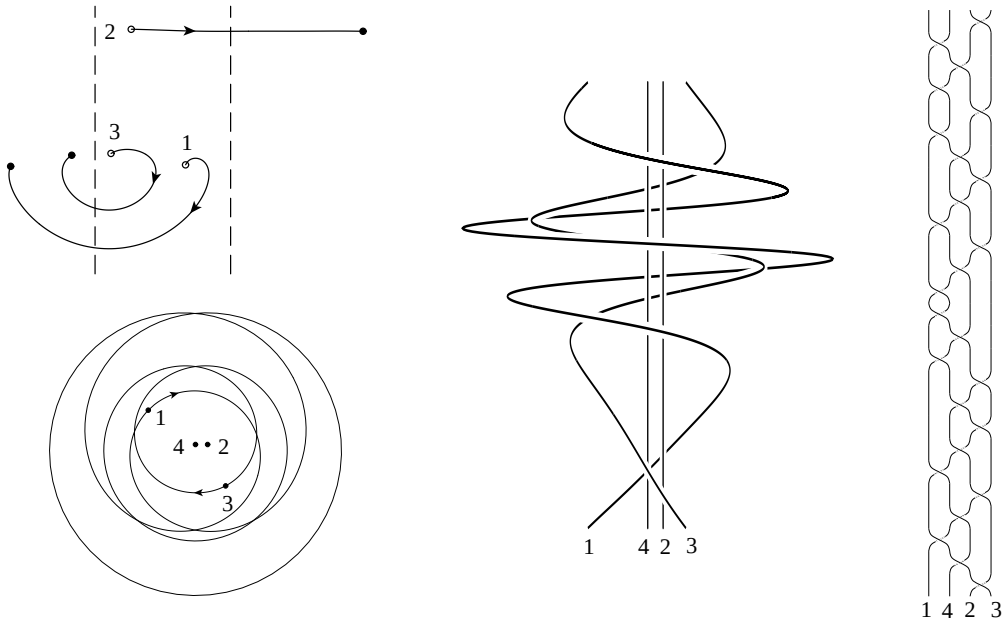

Figure 4.4: Vortex motion from regime II of Figure 3.2. (a) Trajectories of the three vortices in the singly-periodic plane (only one representative of each family is shown). (b) The motion in the frame of the second vortex transformed into the plane. (c) Physical braid of the transformed motion. (d) Mathematical braid of the transformed motion.

be viewed as taking place on a torus with width p in both directions. The generic orbit of this system is a periodic orbit $Z(t)$. This periodic orbit can be used to generate a motion of the three vortices on the torus that is periodic in the frame of one of the vortices. However, in contrast to the array case, this cannot be transformed into a motion on the plane, and so one must record the motion using the braid group of the torus. This group not only has generators corresponding to the switching of two points as in the usual braid group, but it also has generators describing motions that circulate around the meridian and longitude of the torus (see [Bm2]). Thus the braids are more difficult to visualize. However, the basic features of the analysis in the array and plane case go through without difficulty. In particular, each regime is assigned just one braid, and so the braid captures the sense in which all the vortex motions in one regime are topologically the same and distinct from those of other regimes.

§5 Isotopy classes and the Thurston-Nielsen theory.

This section provides an introduction to isotopies and the Thurston-Nielsen theory in preparation for the study of the advection homeomorphisms generated by vortex motions. The material on the Thurston-Nielsen theory is targeted for our applications. We state many results without proof. The reader is urged to consult [T], [FLP], or [CB] for a more balanced and complete treatment. For a survey of the dynamical applications of the Thurston-Nielsen theory, see [Bd].

§5.1 Homeomorphisms, isotopy, and braids.

Most of the homeomorphisms occuring in this paper are defined using the advection of

a passive particle in a time-varying velocity field. Given a perhaps time-dependent vector field on the plane (u, v), the flow line with position z_0 at time t_0 is denoted $z(t; z_0, t_0)$. By convention, the running time t satisfies $z(t_0; z_0, t_0) = z_0$, *not* $z(0; z_0, t_0) = z_0$ (unless, of course, $t_0 = 0$). Fixing a time t, the *time-t flow map* or the *time-t advection homeomorphism* is $h_t(z_0) := z(t; z_0, 0)$. The collection of h_t for all t is called a *fluid motion*.

If E is a finite set and f is a homeomorphism of $\mathbb{R}^2$ with $f(E) = E$, then f is called a *rel E homeomorphism*. Given two rel E homeomorphisms $f_i : \mathbb{R}^2 \to \mathbb{R}^2$, f_0 is *isotopic to f_1 rel E* if they can be connected by a continuous family of rel E homeomorphisms f_t, $t \in [0, 1]$. Since E is a finite set, this implies that $f_t(k) = f_0(k)$ for all t and $k \in E$. The collection of homeomorphisms isotopic to f rel E is called its *rel E isotopy class*. The finite set E in the sequel will be the initial positions of the collection of point vortices. It is sometimes convenient to remove the set E from the plane and consider a rel E homeomorphism as a homeomorphism of the punctured plane $\mathbb{R}^2 - E$. Two rel E homeomorphisms are isotopic rel E exactly when they are isotopic as homeomorphisms of $\mathbb{R}^2 - E$.

The simplest case is isotopy to the identity map. Given a fluid motion h_t, the motion of the points in E is given by $a_i(t) := h_t(k_i)$ for each $k_i \in E$. If h_1 is a rel E homeomorphism, this motion generates a physical braid $\mathbf{b}$ with endpoint set E. The homeomorphism h_1 is isotopic to the identity rel E if and only if the physical braid $\mathbf{b}$ can be deformed into the trivial physical braid, which consists of just vertical strands at the points of E. This is certainly the case when the mathematical braid representing $\mathbf{b}$ is the identity element in the braid group, but this is not the only case. Consider the plane motion given in complex coordinates by $g_t(z) = z \exp(2\pi i t)$. For a given n, let E be the set of n^{th} roots of unity, $\{\exp 2\pi i j/n : j = 1, \ \ldots \ , n\}$. Then it is easy to check that the physical braid $\mathbf{b}$ of the motion of E has a mathematical braid $(\bar{\sigma}_1 \bar{\sigma}_2 \ \ldots \ \bar{\sigma}_{n-1})^n$ and further that $\mathbf{b}$ can be deformed to the trivial braid by just untwisting. It is known that this mathematical braid and its powers are the only cases where this happens ([Bm1]). More precisely, if we let $\hat{B}_n$ be B_n with the added relation that $(\sigma_1 \sigma_2 \ \ldots \ \sigma_{n-1})^n$ is the identity element, then the braid word of $\mathbf{b}$ is equivalent to the identity element of $\hat{B}_n$ exactly when the corresponding rel E advection homeomorphism is isotopic to the identity. Note that the center of B_n (i.e. , all the elements which commute with every other element) is exactly all the powers of $(\sigma_1 \sigma_2 \ \ldots \ \sigma_{n-1})^n$, so one could more succinctly define $\hat{B}_n$ as B_n modulo its center.

In the general case, isotopy can be described using the identity case. Two rel E homeomorphisms f and g are isotopic if there is a third homeomorphism h such that h is isotopic to the identity and $g = h \circ f$. If f and g are time-1 maps of fluid motions, then they are isotopic if we can accomplish the same advection as g by first allowing the advection for f and then following it by a fluid motion that keeps the points of E fixed (infinitesimal rotations about the points of E are allowed). Using the result in the identity case, two rel E advection homeomorphisms are isotopic if and only if the corresponding braid words are equivalent in $\hat{B}_n$. In different language, the collection of rel E isotopy classes forms a group under composition; this group is isomorphic to $\hat{B}_n$, where n is the number of elements in E.

We also need to allow different distinguished sets E so that vortex motions with different initial configurations can be compared. A rel E homeomorphism f and a rel E' homeomorphism f' are *isotopic up to conjugacy* if there is a homeomorphism h such that $h(E') = E$ and $hf'h^{-1}$ is isotopic to f rel E. Thus f and g are isotopic after a change of coordinates. The result here is that two advection homeomorphisms are isotopic up to conjugacy if and only if their mathematical braid words are conjugate in $\hat{B}_n$.

§**5.2 The Thurston-Nielsen representative.** The Thurston-Nielsen theory provides tools to analyse homeomorphisms using their isotopy classes. The theory constructs, in each isotopy class, a special homeomorphism which is now called the *Thurston-Nielsen* (TN) *representative*. This TN-homeomorphism is in a precise sense the simplest map in the isotopy class, simplest in both the topological and dynamical sense. Thus, once we understand the topology and dynamics of the TN-homeomorphism in an isotopy class, we know the dynamical and topological complexity that must be present in *every* homeomorphism in the class.

The TN-homeomorphisms are of three basic types. The first type consists of dynamically very simple maps called *finite order (fo)*. These are defined by the property that, for some $m > 0$, the map composed with itself m times equals the identity map. The second type of TN-homeomorphisms are dynamically very complicated and are called *pseudo-Anosov (pA)* homeomorphisms. These will be discussed in greater detail in the next subsection, because the presence of a pA homeomorphism in an isotopy class has strong implications for the dynamics of an advection homeomorphism. The final type of TN-homeomorphisms are *reducible*, which means that there is a collection of simple disjoint loops with the property that the loops are permuted by the reducible homeomorphism. Cutting along the loops yields a collection of smaller surfaces, and on each of these surfaces, the reducible homeomorphism is either finite order or pA.

A given isotopy class can contain a TN-map of only one type, and thus an isotopy class is called pA, finite-order, or reducible depending on what kind of TN-map it contains. Note that the conjugate of a TN-map is also a TN-map of the same type. Thus, using the results of the previous subsection, one may also speak of the TN-type of a braid or a braid type. There are many theorems that help decide the TN-type of a braid or isotopy class. Rather than catalog these results here, it will suffice to note that there is a computer implementation of an algorithm due to Bestvina and Handel ([BH]) (cf. [FM] and [Ls]) which, given the braid word, decides the TN-type. In the pA case, the algorithm outputs the isotopy invariant dynamical data described in the next subsection.[1]

For planar regions, the finite-order braids and rel E isotopy classes are well known. If we let R_n denote rigid rotation of the plane by $-2\pi/n$, then certainly $R_n^n = id$, and so R_n is finite order. We may consider R_n as the time-1 flow map of the motion given in complex coordinates by $h_t(z) = -z\exp(2\pi it/n)$. If E is the set of n^{th} roots of unity, then its mathematical braid under this motion is $\beta_n := \sigma_1\sigma_2\ \ldots\ \sigma_{n-1}$. Note that β_n^n is the identity element of $\hat{B}_n$, and making this property hold is, in fact, the defining feature of $\hat{B}_n$. Thus, β_n is a finite order braid and so is β_n^m for any $0 \le m \le n-1$. A classic result of Brouwer (see section 8.2 in [Bd]) says that all finite order homeomorphisms of the plane are conjugate to rigid rotations. This implies that the β_n^m are the only finite-order braids on n strands.

For planar regions, the Thurston-Nielsen theory only has content for regions that have three or more punctures or holes, or equivalently, for isotopy classes rel three or more points. When E contains just two points, all TN-homeomorphisms are finite order, since $\hat{B}_2$ only contains the identity element e and the braid σ_1 with $\sigma_1^2 = e$. The classic results of Alexander (see Chapter XV in [D]) say that when E has one or zero elements, there is only one isotopy class; all orientation-preserving homeomorphisms of the plane are isotopic, as are those of

[1] There is a C++ implementation of this algorithm by Toby Hall (with a Windows interface) available for download. Contact the first author for site locations.

the once-punctured plane.

§5.3 Pseudo-Anosov maps and isotopy classes. Linear Anosov maps on tori (such as Arnol'd's cat map) are one of the best known and understood examples of chaotic dynamics. Pseudo-Anosov maps are a generalization that can exist on other surfaces such as the punctured disk. They share many of the properties of linear Anosov maps. A pA map ϕ has uniform expansion and contraction at each point by a factor λ. There is a Markov partition with transition matrix M that allows one to encode the dynamics of the pA map ϕ. The largest eigenvalue of M is the stretching factor $\lambda > 1$ and the number of fixed points of ϕ^n grows like λ^n. The precise way in which these properties are shared by any isotopic map is described a theorem of Handel ([H]). The notation $g_{|Y}$ means the map g restricted to the set Y.

Theorem. *If $\phi : S \to S$ is a pA homeomorphism on a closed surface S and g is isotopic to ϕ, then there exists a closed, g-invariant set Y, and a continuous, onto map $\alpha : Y \to M^2$, so that $\alpha \circ g_{|Y} = \phi \circ \alpha$. Further, for any periodic point x of ϕ, there is a periodic point of the same period y of g with $\alpha(y) = x$.*

Thus, any map g that is isotopic to a pA map has a compact invariant set that is semiconjugate to the pA map. Since the map α is onto, the dynamics of g are at least as complicated as those of the pA map ϕ. Thus, for example, the exponential growth rate of the number of fixed points of g^n is at least λ, and the topological entropy of g is greater than or equal to $\log(\lambda)$. Note that nothing prevents the dynamics of g from being more complicated than that of ϕ; the theory merely provides a lower bound.

A loop in a surface is called *topologically nontrivial* if it cannot be deformed into a point, a puncture, or a boundary component. Another basic result about pA maps is that the length of topologically nontrivial loops grows like λ^n under iteration. Via the semiconjugacy, this implies a similar growth under g. It is important to note that this does not imply that the map g has Lyapunov exponents equal to $\log(\lambda)$ everywhere. One does obtain from smooth ergodic theory that g has an ergodic invariant measure with an exponent at least $\log(\lambda)$ (cf. [KH]), but this measure is supported on the set Y, which could be small with respect to the usual measure on S.

Since the number λ can be computed by the Bestvina-Handel algorithm, the braid describing an isotopy class yields quantitative information about any homeomorphism in the isotopy class. The Bestvina-Handel algorithm also returns a one-dimensional graph called a *train track* in addition to a self-transformation of the graph. The edges of the graph form the Markov partition for the pA map, and the self-transformation of the graph provides the transition matrix as well as the structure of the invariant foliations. These foliations are sometimes called the "invariant manifold template" of the pA map. The semiconjugacy then gives a lower bound or skeleton for the invariant manifold templates of g.

§6 Advection and isotopy classes.

§6.1 The Poincaré map. A vortex motion $z_\alpha(t)$ can be obtained by solving (2.1) directly, or as in §3, by using (3.4) and a period-P solution $Z(t)$ of the reduced equations (3.5). The vortex motion, in turn, generates a velocity field given by the right hand side of (2.3). The goal of this subsection is to define a Poincaré map whose iterates describe the time evolution of passive particles advected in this velocity field. There is a standard construction for periodic velocity fields. It needs to be altered slightly for advection caused by point vortices

because the vortex trajectories satisfy $z_\alpha(t+P) = z_\alpha(t) + b$, where b is the dynamic phase associated with $Z(t)$. The easiest alteration is to pass to a uniformly translating frame with velocity b/P. If $F(z,t)$ denotes the right hand side of (2.3) corresponding to the given vortex motion, define the *advection homeomorphism* f as the time-P flow map of the equation

$$\dot{\zeta} = F\left(\zeta + \frac{b}{P}t, t\right) - \frac{b}{P}.$$

Thus the advection homeomorphism satisfies $f^n(z_0) = z(nP; z_0, 0) - nb$, and so f describes the position of a particle after advecting for one period P and then translating by $-b$. Alternatively, this could have been taken as the definition of f, i.e. , $f(z_0) = z(P; z_0, 0) - b$ with z the solution of (2.3). Points that are periodic under f correspond to advected particles that are translated along with the vortices, but after some integer multiple of P they have returned to their initial positions relative to the vortices. Although the velocity field is not defined at the positions of the vortices, the homeomorphism f can be extended (continuously, not differentially) to make the three initial positions of the vortices, $z_\alpha(0)$, fixed points.

In §4.3, the motion of a vortex array in the cylinder was transformed to the plane minus the origin by the conformal map T. The advection homeomorphism in this case is transformed to $\hat{f} = TfT^{-1}$. Note that $\hat{f}$ may be extended to make 0 a fixed point. Thus all the $s_\alpha(0)$ from (4.4) can be considered as fixed points of $\hat{f}$.

§**6.2 The TN type of regimes.** As seen in §4.2 and §4.4, all the periodic orbits in the same regime in the reduced plane give rise to the same braid. By results in §4.1, this implies that all the corresponding advection homeomorphisms have the same braid type, which allows us to speak of the TN type of a regime. If this type is pA, then, as in §5.3, all the advection homeomorphisms share a certain set of dynamics.

In the case of three vortices in the plane, only two braid types arise as descriptions of regimes. In one of them, a pair of vortices rotates around one other while the other vortex is uninvolved. This is a reducible class, with a finite-order component containing the pair of interacting vortices. The other regime, D, has braid $(\sigma_1\sigma_2)^3$, which is the identity element in $\hat{B}_3$, and the advection homeomorphism in this case is isotopic to the identity, where the isotopy consists of unwrapping the plane via single rotation; this topologically undoes whatever advection is caused by the vortices. Since only pA classes or components yield dynamical information from the Thurston-Nielsen theory, the theory does not imply chaotic advection dynamics in the planar case. This means that any chaotic advection is caused by something other than the topology of the vortex motions (see the conclusion for further related discussion).

The Thurston-Nielsen theory does provide dynamical information about advection induced by vortex arrays. The Bestvina-Handel algorithm was used to compute the TN type of the various regimes from Figure 3.2. Using the braids given in the second column as input, the computed TN type is shown in the third column of Table 4.1. When a regime is pA (or has a pA component), the expansion constant is given in the right column.

The regimes that contain poles, III through VIII, correspond to a pair of vortices which rotates around one other while the other is uninvolved. As in the planar case, the isotopy classes of the advection homeomorphisms are reducible with a finite-order component that contains the pair of interacting vortices.

In the braid for regime X shown in Figure 6.1a, the three rightmost strands do not link with the leftmost string. This shows that the corresponding isotopy class is reducible with

a reducing circle that contains the three rightmost strands. Inside this reducing circle, the behavior as a *three*-braid is $\sigma_2\sigma_1\sigma_2\sigma_1\sigma_2\sigma_1 = (\sigma_1\sigma_2)^3$, using the relations in B_3. This braid is the same as the braid for region D in the planar case, which represents the identity class. Thus, for regime X, the isotopy classes are reducible with all finite-order components. The braid for regime IX is reducible in a way similar to that of regime X, but inside the reducing circle, the class is again reducible, but still with all finite order components.

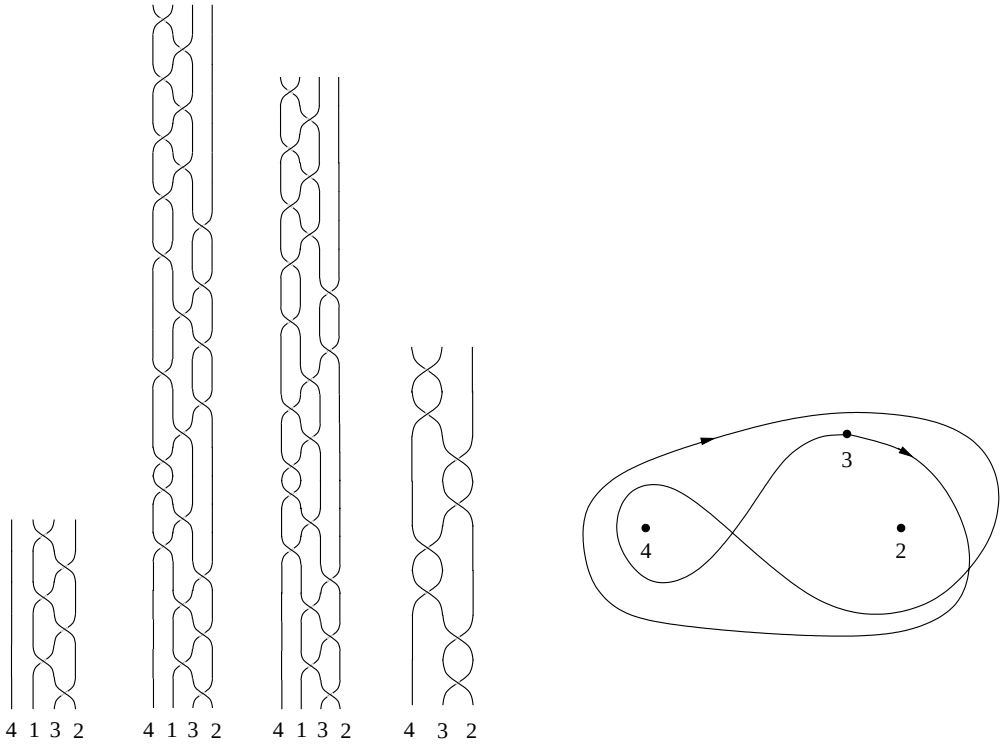

Figure 6.1: Mathematical braids of regimes from Figure 3.2: (a) Regime X; (b) Regime XII; (c) Regime XI. The braid of regime XI restricted to vortices 2, 3, and 4 is shown in (d), and a schematic illustration of the plane motion of the vortices is shown in (e).

The braid for regime II is shown in Figure 4.4d. The schematic of the plane motion in Figure 4.4b makes it clear that the class is reducible; one can enclose the motions in successive, nested reducing curves. The classes for regime I are similar.

The braid for regime XII is shown in Figure 6.1b. The braid makes it clear that vortices 1 and 3 have essentially the same motion with respect to vortex 2 and the origin ("vortex" 4). They do rotate around each other once, but they may be enclosed in a reducing circle. To analyze the class outside the reducing circle, we think of squeezing the strands of vortices 1 and 3 into a single strand, or equivalently, we delete one of the strands. The result is the three-braid $\sigma_2^2\sigma_1^2\sigma_2^2\bar{\sigma}_1^2$ shown in Figure 6.1d. This braid corresponds to a pA class rel 3 points with $\lambda \approx 13.9$.

Regime XI also yields a pA class with $\lambda \approx 13.9$. Although this class is irreducible, the strand corresponding to vortex 1 is in fact a fixed point of the pA map in the class defined by the other three strands. The latter is the same as that for regime XII (see Figure 6.1). The dynamics in regime XI is considered in detail in the next subsection. The last regime is

XIII, which is pA with $\lambda \approx 9.9$.

§6.3 An example of the dynamical implications of the Thurston-Nielsen theory. As an example, we describe some of the results afforded by the Thurston-Nielsen theory for advection homeomorphisms coming from vortex motions in regime XI. Similar conclusions apply to other regimes of pA type, with the numerical value of the appropriate stretching coefficient λ substituted for the $\lambda \approx 13.9$ that holds in regime XI. Begin by fixing a periodic orbit $Z(t)$ in regime XI and an initial position $z_1(0)$ and thus obtain a motion of all the vortices as in §6.1. The corresponding advection homeomorphism is denoted f. We may variously consider f as a homeomorphism of the singly-periodic plane, the cylinder, or as transformed from the cylinder to the plane by the conformal map T.

Using the theorem of §5.3 and the comments after it, we know that the number of fixed points of f^n grows with n at least like 13.9^n. These fixed points for f^n correspond in the lab frame to passive particles that are advected by the vortex velocity field and after n periods have returned to the same position *relative to the vortex array*. We also know that, under advection, topologically nontrivial curves grow in length at least at a rate of 13.9^n. In addition, the topological entropy of f is at least $\log(13.9)$. This implies that f has a hyperbolic invariant measure (in the sense of [KH]) with Lyapunov exponents $\log(13.9)$, but no information is available regarding its support.

As noted at the end of §4.2, although all the advection homeomorphisms arising from vortex motions in regime XI have these properties, the time scale of the advection described by the homeomorphism varies greatly among motions in the same regime. In addition, variations in the dynamic phase make a significant difference in the motion as observed in the lab frame.

The picture of the trajectories of the vortices transformed into the plane is also instructive. Figure 6.1c shows the mathematical braid of this regime. Figure 6.1d shows just the motion of vortices 3 and 2 and the origin (i.e. , "vortex" 4), while Figure 6.1e shows a schematic of this motion in the frame of vortex 2 after it has been transformed to the plane. The feature of note is that the trajectory of vortex 3 crosses itself in an essential way. We cannot remove this self-intersection by deforming the path in the complement of vortex 2 and the origin. This essential self intersection in fact implies that the isotopy class of the advection homeomorphism generated by vortex 3, vortex 2, and the origin is pA. The self-intersection forces regions of the fluid to be repeatedly pushed across pieces of themselves as they are advected. This forces the advection homeomorphism to constantly stretch and fold in an essential topological fashion. It is well known that stretching and folding is a basic mechanism for the generation of chaos, and in this case, it is topological in nature and is present in any map in the isotopy class.

§7 Discussion and conclusions.

The geometric and topological methods in this paper have illuminated many aspects of the dynamics of three-vortex systems with zero net circulation. Using reduction, the vortex systems were mapped onto one-degree-of-freedom (*dof*) Hamiltonian systems. These Hamiltonian systems have a natural subdivision into regimes, and all the solutions corresponding to a single regime yield topologically identical vortex motions as described by braids. Thus, the braid of a vortex motion provides a precise topological way of distinguishing and describing the motion in various regimes. Further, the constancy of the braid over a regime indicates a topological stability of the dynamics over a range of initial conditions. For three vortices

in the infinite plane, the braid description shows that regimes are characterized essentially by which pair of vortices rotate around one another. In the vortex array example, there is a much richer collection of braids, indicating a wide assortment of topological motions of the vortices.

The braid of a vortex motion not only describes the topology of the motion but also provides data that characterizes the isotopy class of the advection homeomorphism induced in the surrounding fluid. In the array example, there are advection homeomorphisms whose isotopy classes are of pA type. Theorems from the Thurston-Nielsen theory thus imply that the advection dynamics is chaotic and provide quantitative lower bounds for the chaos for each such regime. It is important to note that this information comes not from a perturbation of a regular motion, but rather results from advection dynamics that is chaotic in a global, topological sense (a detailed discussion of connections to Melnikov theory is contained in [BAS]). In the pA case, Handel's theorem yields a set Y present in the fluid on which the dynamics is chaotic in the strongest sense: there is a coding by a subshift of finite type and there is an ergodic invariant measure supported on Y which has positive Lyapunov exponents and positive metric entropy. Furthermore, the theorem shows how this dynamics is topologically embedded in the fluid.

Such strong conclusions from limited data naturally raise the question of the dependence of the results on the specifics of the systems analyzed here. In addition, what are the implications and expectations for more general vortex systems, and what do the results say about two-dimensional fluid flows in general?

First note that the examples chosen represent the "generic" case within the class of three-vortex systems with zero net circulation. In the infinite plane, except for a few degenerate cases, changing the values of the circulations does not change the basic structure of the reduced systems and corresponding braids (see [Af2]). For arrays and lattices as Γ_3 moves down the Farey tree (fixing $\Gamma_1 = 1$), the number of regimes and the complication of their braids increases dramatically (see [AS] and [SA]). We have examined a number of cases and have consistently found pA regimes after one has moved sufficiently down the tree.

The next issue is the dependence of the results on having zero net circulation and $N = 3$ vortices. The Poisson bracket of the two components of the linear impulse, P and Q, is equal to the net circulation of a vortex system. Thus when the net circulation is zero, the integrals are in involution, and so the vortex system can be reduced by 2 *dof* (or 4 dimensions). Since each vortex contributes one *dof*, for three vortices, we obtain a one-degree-of-freedom Hamiltonian system. The two dimensionality of this system allows us to define regimes and their braids. If there is non-zero net circulation or more than three vortices, reduction yields a Hamiltonian system with more than one *dof*.[1] Such systems do not have a nice subdivision into regimes and usually most orbits (in terms of measure or probability) are not periodic. Thus a simple-minded application of the methods of this paper fails. However, except in very exceptional cases, high-degree-of-freedom Hamiltonian systems have an abundance of periodic orbits, and the expectation is that most orbits (in terms of topology) are periodic. Each such periodic orbit of the reduced system represents a motion of the collection of vortices that is periodic up to a dynamic phase. For these periodic motions, the topological

[1] In planar vortex systems the angular impulse, $\sum \Gamma_\alpha |z_\alpha|^2$, is always in involution with $|J|^2$. This allows a reduction by two *dof* for these systems even when the net circulation is nonzero.

analysis used here goes through with little change. We expect that in the high-degree-of-freedom case, there will be an abundance of periodic orbits yielding pA classes and, thus, topologically chaotic advection.

While periodicity is not the typical behavior (in terms of measure) in high-degree-of-freedom Hamiltonian systems, recurrence is typical. If the vortex paths corresponding to a recurrent orbit cross each other in topologically nontrivial ways, it is clear that the same mechanisms operate on the surrounding fluid, regardless of whether the vortices return exactly to their initial positions or not. Material patches of the fluid are pulled across the paths of other vortices and stretched, and the process is repeated, yielding exponential stretching. Unfortunately, the mathematical theory for obtaining rigorous conclusions about isotopy relative to recurrent but non-periodic orbits is not yet fully developed. One approach is to take the closure of an orbit (for a homeomorphism of the plane) and study isotopy classes relative to that compact invariant set ([BdHl] and [HM]). Another approach is to close the orbit after some long time and then apply the theory. This follows work of Arnol'd ([A3]) and Fried ([F]) and this idea has been used by Gambaudo and Pécou ([GP]) to obtain a braid-valued cocycle that yields asymptotic lower bounds for the dynamical complexity. These mathematical questions and their applications to vortex systems are a promising area for future research. At this point it seems clear that, in general, many vortex systems will be more complex than the examples studied here and thus will exhibit pA-type behavior in abundance (cf. [ABSV]).

The first observations on the implications of our methods and results for more general two-dimensional fluid flows come from the usual interpretations and applications of the point vortices as approximations to regions of concentrated vorticity. The motion of these regions is determined primarily by interactions with other vortex patches. Thus, the motion of the point vortices can be identified with large-scale motions. The braid description gives a precise meaning to the topology of the large scales and could equally well be applied to the motion of vortex patches. The notion of reducibility of a braid precisely describes topological hierarchies within the large scale motions. After understanding the large-scale self-interactions one wants to know their influence on the ambient fluid motion. Within the point vortex framework, this influence is modeled by the advection homeomorphisms. The influence of the large scales on the topology of the fluid motion is thus discerned from the braids, because they provide the combinatorial data that characterizes the isotopy class of the advection homeomorphism. The Thurston-Nielsen theory takes this data and returns quantitative and topological information about the advection dynamics. Thus, the theory provides detailed dynamical information about the fluid motion from combinatorial, topological data about the motion of the large scales.

In addition to point vortices and vortex patches, there are other fluid models, such as moving boundaries and "Stokelets" in Stokes flow, in which the fluid motion is induced by large-scale motions which are themselves determined only by self-interactions or else by external driving. These models are usually studied from a primarily Eulerian perspective, i.e., the velocity field generated in the fluid by the autonomous large scales is the focus of attention. In contrast, the methods of this paper treat all such objects as stirrers; we consider only the effect on the fluid arising from their displacement of the fluid. Thus, the large scales here are viewed strictly from a Lagrangian viewpoint: we focus on their motion and its effect on fluid trajectories and the motion of material patches in the fluid. We have seen that if the topology of "stirrer" motions is complicated enough, it always results in

exponential stretching and the related chaotic dynamics.

It is clear that, in most models, and indeed in a two-dimensional fluid, it is important to understand both the Eulerian and Lagrangian aspects of the large-scale motions. In certain cases, their relative importance is easy to ascertain. For example, in the planar systems of vortices considered here, the advection isotopy classes are all of finite order type and so the pA stirring mechanism is absent, and thus any chaotic advection has other causes. On the other hand, in the mixing of a viscous fluid studied in [BAS], when the rods are moved in a protocol resulting in an advection homeomorphism in a pA isotopy class, one clearly sees the structure and result of the pA map. Thus, the stirring mechanism clearly dominates. In contrast, a finite order stirring protocol results in spiral patterns for advected scalars and apparently lacks chaotic advection. In another example studied in [AB], rods placed in a viscous fluid are rotated and not translated. This procedure results in trivial isotopy classes. Nonetheless, there is chaotic advection for certain rotation schemes, and this chaotic dynamics must arise from something other than a pA stirring mechanism.

We have seen that in certain cases, the Thurston-Nielsen theory provides a way to precisely determine the influence of the topological kinematics of the large scales on the dynamics of the surrounding fluid motions. The importance of the topology of the large-scale motions in more realistic situations, such as the motion of regions of concentrated vorticity in decaying two-dimensional turbulence, needs to be determined. But in studying the Lagrangian motions of fluid particles, it is clearly valuable to study the Lagrangian motions of the large scales, and the methods of this paper provide topological tools for this endeavor.

References

[AM] Abraham, R. and Marsden, J.E., *Foundations of Mechanics*, Addison-Wesley, 1985.

[AR] Adams, M. and Ratiu, T., The three-point vortex problem: commutative and noncommutative integrability, *Contemporary Mathematics*, **81**, 1988, 245–257.

[Af1] Aref, H., Integrable, chaotic and turbulent vortex motion in two-dimensional flows, *Ann. Rev. Fluid Mech.*, **15**, 1983, 345-389.

[Af2] Aref, H., Three-vortex motion with zero total circulation: Addendum (Addendum to paper by N. Rott), *J. Appl. Math. Phys. (ZAMP)*, **40**, 1989, 495–500.

[AB] Aref, H.; Balachandar, S. Chaotic advection in a Stokes flow. Phys. Fluids 29 (1986), no. 11, 3515–3521.

[ABSV] Aref, H., Boyland, P., Stremler, M., and Vainchtein, D., Turbulent statistical mechanics of systems of point vortices, *Fundamental problematic issues in turbulence (Monte Verita, 1998)*, *Trends in Mathematics*, Birkhäuser, Basel, 1999, 151–161.

[AS] Aref, H. and Stremler, M. A., On the motion of three point vortices in a periodic strip, *J. Fluid Mech.*, **314**, 1996, 1–25.

[AN] Aref, H., Newton, P.K., Stremler, M., Tokieda, T., Vainchtein,D., Vortex crystals, *Adv. Appl. Mech.*, **39**, in press.

[A1] Arnol'd, V. I., Remarks on quasicrystallic symmetries, *Phys. D*, **33**, 1988, 21–25.

[A2] Arnol'd, V. I., *Mathematical methods of classical mechanics*, Springer-Verlag, 1989.

[AK] Arnol'd, V. I. and Khesin, B., *Topological methods in hydrodynamics*, Applied Mathematical Sciences, **125**, Springer-Verlag, 1998.

[A2] Arnol'd, V. I., The asymptotic Hopf invariant and its applications, translationed in *Selecta Math. Soviet*, **5**, 1986, 327–345.

[BH] Bestvina, M. and Handel, M., Train tracks for surface homeomorphisms, *Topology*, **34**, 1995, 109–140.

[Bm1] Birman, J, *Braids, Links and Mapping Class Groups*, Annals of Mathematics Studies, Princeton University Press, 1975.

[Bm2] Birman, J., On braid groups, *Com. Pure and Appl. Math.*, **22**, 1969, 41–72.

[BL] Birman, J. and Libgober, A., ed., Proceedings of the AMS-IMS-SIAM Joint Summer Research Conference on Artin's Braid Group, *Contemp. Math.*, **78**, 1988.

[Bd] Boyland, P. Topological methods in surface dynamics, *Topology and its Applications*, **58**, 223–298, 1994.

[BAS] Boyland, P., Aref, H. and Stremler, M., Topological fluid mechanics of stirring, *J. Fluid Mech.*, **403**, 277–304, 2000.

[BdHl] Boyland, P. and Hall, T., Isotopy stable dynamics relative to compact invariant sets, *Proceedings London Math. Soc.*, **79**, 673–693, 1999.

[CB] Casson, A. and Bleiler, S., *Automorphisms of Surfaces after Nielsen and Thurston*, London Math. Soc. Stud. Texts, **9**, Cambridge University Press, 1988.

[C1] Chorin, A. J., Turbulence and vortex stretching on a lattice, *Commun. Pure Appl. Math.*, **39** (Supplement), 1986, S47–S65.

[C2] Chorin, A. J., Scaling laws in the vortex lattice model of turbulence, *Commun. Math. Phys.*, **114**, 1988, 167–176.

[C3] Chorin, A. J., Spectrum, dimension, and polymer analogies in fluid turbulence, *Phys. Rev. Lett.*, **60**, 1988, 1947–1949.

[D] Dugundji, J., *Topology*, Allyn and Bacon, Inc., 1966.

[FLP] Fathi, A., Lauderbach, F. and Poenaru, V., Travaux de Thurston sur les surfaces, *Asterique*, **66-67**, 1979.

[FM] Franks, J. and Misiurewicz, M., Cycles for disk homeomorphisms and thick trees, *Contemp. Math.*, **152**, 1993, 69–139.

[F] Fried, D., The geometry of cross sections to flows, *Topology*, **24**, 353–371, 1983.

[GP] Gambaudo, J.-M.; Pécou, E. E., Dynamical cocycles with values in the Artin braid group, *Ergodic Theory Dynam. Systems*, **19**, 1999, 627–641.

[G] Gilbert, A., Towards a realistic fast dynamo: models based on cat maps and pseudo-Anosov maps, *Proc. Roy. Soc. London*, Ser. A, **443**, 1993, 585–606.

[H] Handel, M., Global shadowing of pseudo-Anosov homeomorphisms, *Ergod. Th. & Dynam. Sys.*, **5**, 1985, 373–377.

[HM] Handel, M. and Miller, R., End periodic homeomorphisms, handwritten manuscript, 1985.

[J] Janot, C., *Quasicrystals: a primer*, Oxford University Press, 1992.

[K] Kirchhoff, G. R., *Vorlesungen über Mathematische Physik, Mechanik*, Teubner, 1877.

[KH] Katok, A. and Hasselblat, B., *Introduction to the modern theory of dynamical systems*, Cambridge University Press, 1995.

[L] Leonard, A., Computing three-dimensional incompressible flows with vortex elements, *Ann. Rev. Fluid Mech.*, **17**, 1985, 523–559.

[Ls] Los, J., Pseudo-Anosov maps and invariant train tracks in the disc: a finite algorithm, *Proc. London Math. Soc.*, **66**, 400–430, 1993.

[McT] McRobie, F. A. and Thompson, J. M. T., Braids and knots in driven oscillators, *Intern. J. Bifurcation & Chaos*, **3**, 1993, 1343–1361.

[Mj] Majda, A. J., Vorticity, turbulence, and acoustics in fluid flow, *SIAM Rev.*, **33**, 1991, 349–388.

[M] J. Marsden *Lectures on Mechanics*, LMS Lecture Note Series, **174**, Cambridge University Press, 1992.

[MH] Meyer, K.R. and Hall, G.R., *Introduction to Hamiltonian Dynamical Systems and the N-Body Problem*, Springer-Verlag, 1992.

[MfT1] Moffatt, H. K. and Tsinober, A., eds., *Topological fluid mechanics*, Proceedings of the IUTAM Symposium held in Cambridge, August 13–18, 1989, Cambridge University Press, Cambridge, 1990.

[MfT2] Moffatt, H. K. and Tsinober, A., Helicity in laminar and turbulent flow, *Ann. Rev. Fluid Mech.*, **24**, 1992, 281–312.

[Mt] Montgomery, R., The N-body problem, the braid group, and action-minimizing periodic solutions, *Nonlinearity*, **11**, 1998, 363–376.

[Mo] Moore, C., Braids in classical dynamics, *Phys. Rev. Lett.*, **70**, 3675–3679, 1993.

[O] O'Neil, K. A., On the Hamiltonian dynamics of vortex lattices, *J. Math. Phys.*, **30**, 1989, 1373–1379.

[PM] Pekarsky, S. and Marsden, J., Point vortices on a sphere: stability of relative equilibria, *J. Math. Phys.*, **39**, 1998 5894–5907.

[PS] Pullin, D. I. and Saffman, P. G., Vortex dynamics in turbulence, *Ann. Rev. Fluid Mech.*, **30**, 1998, 31–51.

[Ri] Ricca, R. (ed) *An Introduction to the Geometry and Topology of Fluid Flows*, Kluwer Academic Publishers, 2001.

[S] Saffman, P. G., Dynamics of vorticity, *J. Fluid Mech.*, **106**, 1981, 49–58.

[SB] Saffman, P. G. and Baker, G. R., Vortex interactions, *Ann. Rev. Fluid Mech.*, **11**, 1979, 95–122.

[Srp] Sarpkaya, T., Computational methods with vortices - The 1988 Freeman Scholar lecture, *J. Fluids Engin.*, **111**, 1989, 5–52.

[SL] Shariff, K. and Leonard, A., Vortex rings, *Ann. Rev. Fluid Mech.*, **24**, 1992, 235–279.

[SA] Stremler, M. A. and Aref, H., Motion of three point vortices in a periodic parallelogram, *J. Fluid Mech.*, **392**, 1999, 101–128.

[T] Thurston, W., On the geometry and dynamics of diffeomorphisms of surfaces, *Bull. A.M.S.*, **19**, 417–431, 1988.

[Z] Zabusky, N. J., Computational synergetics and mathematical innovation, *J. Comp. Phys.*, **43**, 1981, 195–249.

List of Recent TAM Reports

No.	Authors	Title	Date
928	Thoroddsen, S. T., and K. Takehara	The coalescence–cascade of a drop—*Physics of Fluids* **12**, 1257–1265 (2000)	Feb. 2000
929	Liu, Z.-C., R. J. Adrian, and T. J. Hanratty	Large-scale modes of turbulent channel flow: Transport and structure—*Journal of Fluid Mechanics* **448**, 53–80 (2001)	Feb. 2000
930	Borodai, S. G., and R. D. Moser	The numerical decomposition of turbulent fluctuations in a compressible boundary layer—*Theoretical and Computational Fluid Dynamics* (submitted)	Mar. 2000
931	Balachandar, S., and F. M. Najjar	Optimal two-dimensional models for wake flows—*Physics of Fluids*, in press (2000)	Mar. 2000
932	Yoon, H. S., K. V. Sharp, D. F. Hill, R. J. Adrian, S. Balachandar, M. Y. Ha, and K. Kar	Integrated experimental and computational approach to simulation of flow in a stirred tank—*Chemical Engineering Sciences* **56**, 6635–6649 (2001)	Mar. 2000
933	Sakakibara, J., Hishida, K., and W. R. C. Phillips	On the vortical structure in a plane impinging jet—*Journal of Fluid Mechanics* **434**, 273–300 (2001)	Apr. 2000
934	Phillips, W. R. C.	Eulerian space–time correlations in turbulent shear flows—*Physics of Fluids* **12**, 2056–2064 (2000)	Apr. 2000
935	Hsui, A. T., and D. N. Riahi	Onset of thermal–chemical convection with crystallization within a binary fluid and its geological implications—*Geochemistry, Geophysics, Geosystems* **2**, 2000GC000075 (2001)	Apr. 2000
936	Cermelli, P., E. Fried, and S. Sellers	Configurational stress, yield, and flow in rate-independent plasticity—*Proceedings of the Royal Society of London A* **457**, 1447–1467 (2001)	Apr. 2000
937	Adrian, R. J., C. Meneveau, R. D. Moser, and J. J. Riley	Final report on 'Turbulence Measurements for Large-Eddy Simulation' workshop	Apr. 2000
938	Bagchi, P., and S. Balachandar	Linearly varying ambient flow past a sphere at finite Reynolds number—Part 1: Wake structure and forces in steady straining flow	Apr. 2000
939	Gioia, G., A. DeSimone, M. Ortiz, and A. M. Cuitiño	Folding energetics in thin-film diaphragms—*Proceedings of the Royal Society of London A* **458**, 1223–1229 (2002)	Apr. 2000
940	Chaïeb, S., and G. H. McKinley	Mixing immiscible fluids: Drainage induced cusp formation	May 2000
941	Thoroddsen, S. T., and A. Q. Shen	Granular jets—*Physics of Fluids* **13**, 4–6 (2001)	May 2000
942	Riahi, D. N.	Non-axisymmetric chimney convection in a mushy layer under a high-gravity environment—In *Centrifugal Materials Processing* (L. L. Regel and W. R. Wilcox, eds.), 295–302 (2001)	May 2000
943	Christensen, K. T., S. M. Soloff, and R. J. Adrian	PIV Sleuth: Integrated particle image velocimetry interrogation/validation software	May 2000
944	Wang, J., N. R. Sottos, and R. L. Weaver	Laser induced thin film spallation—*Experimental Mechanics* (submitted)	May 2000
945	Riahi, D. N.	Magnetohydrodynamic effects in high gravity convection during alloy solidification—In *Centrifugal Materials Processing* (L. L. Regel and W. R. Wilcox, eds.), 317–324 (2001)	June 2000
946	Gioia, G., Y. Wang, and A. M. Cuitiño	The energetics of heterogeneous deformation in open-cell solid foams—*Proceedings of the Royal Society of London A* **457**, 1079–1096 (2001)	June 2000
947	Kessler, M. R., and S. R. White	Self-activated healing of delamination damage in woven composites—*Composites A: Applied Science and Manufacturing* **32**, 683–699 (2001)	June 2000

List of Recent TAM Reports (cont'd)

No.	Authors	Title	Date
948	Phillips, W. R. C.	On the pseudomomentum and generalized Stokes drift in a spectrum of rotational waves—*Journal of Fluid Mechanics* **430**, 209–229 (2001)	July 2000
949	Hsui, A. T., and D. N. Riahi	Does the Earth's nonuniform gravitational field affect its mantle convection?—*Physics of the Earth and Planetary Interiors* (submitted)	July 2000
950	Phillips, J. W.	Abstract Book, 20th International Congress of Theoretical and Applied Mechanics (27 August – 2 September, 2000, Chicago)	July 2000
951	Vainchtein, D. L., and H. Aref	Morphological transition in compressible foam—*Physics of Fluids* **13**, 2152–2160 (2001)	July 2000
952	Chaïeb, S., E. Sato-Matsuo, and T. Tanaka	Shrinking-induced instabilities in gels	July 2000
953	Riahi, D. N., and A. T. Hsui	A theoretical investigation of high Rayleigh number convection in a nonuniform gravitational field—*Acta Mechanica* (submitted)	Aug. 2000
954	Riahi, D. N.	Effects of centrifugal and Coriolis forces on a hydromagnetic chimney convection in a mushy layer—*Journal of Crystal Growth* **226**, 393–405 (2001)	Aug. 2000
955	Fried, E.	An elementary molecular-statistical basis for the Mooney and Rivlin–Saunders theories of rubber-elasticity—*Journal of the Mechanics and Physics of Solids* **50**, 571–582 (2002)	Sept. 2000
956	Phillips, W. R. C.	On an instability to Langmuir circulations and the role of Prandtl and Richardson numbers—*Journal of Fluid Mechanics* **442**, 335–358 (2001)	Sept. 2000
957	Chaïeb, S., and J. Sutin	Growth of myelin figures made of water soluble surfactant—Proceedings of the 1st Annual International IEEE–EMBS Conference on Microtechnologies in Medicine and Biology (October 2000, Lyon, France), 345–348	Oct. 2000
958	Christensen, K. T., and R. J. Adrian	Statistical evidence of hairpin vortex packets in wall turbulence—*Journal of Fluid Mechanics* **431**, 433–443 (2001)	Oct. 2000
959	Kuznetsov, I. R., and D. S. Stewart	Modeling the thermal expansion boundary layer during the combustion of energetic materials—*Combustion and Flame*, in press (2001)	Oct. 2000
960	Zhang, S., K. J. Hsia, and A. J. Pearlstein	Potential flow model of cavitation-induced interfacial fracture in a confined ductile layer—*Journal of the Mechanics and Physics of Solids*, **50**, 549–569 (2002)	Nov. 2000
961	Sharp, K. V., R. J. Adrian, J. G. Santiago, and J. I. Molho	Liquid flows in microchannels—Chapter 6 of *CRC Handbook of MEMS* (M. Gad-el-Hak, ed.) (2001)	Nov. 2000
962	Harris, J. G.	Rayleigh wave propagation in curved waveguides—*Wave Motion* **36**, 425–441 (2002)	Jan. 2001
963	Dong, F., A. T. Hsui, and D. N. Riahi	A stability analysis and some numerical computations for thermal convection with a variable buoyancy factor—*Journal of Theoretical and Applied Mechanics*, in press (2002)	Jan. 2001
964	Phillips, W. R. C.	Langmuir circulations beneath growing or decaying surface waves—*Journal of Fluid Mechanics* (submitted)	Jan. 2001
965	Bdzil, J. B., D. S. Stewart, and T. L. Jackson	Program burn algorithms based on detonation shock dynamics—*Journal of Computational Physics* (submitted)	Jan. 2001
966	Bagchi, P., and S. Balachandar	Linearly varying ambient flow past a sphere at finite Reynolds number: Part 2—Equation of motion—*Journal of Fluid Mechanics* (submitted)	Feb. 2001
967	Cermelli, P., and E. Fried	The evolution equation for a disclination in a nematic fluid—*Proceedings of the Royal Society A* **458**, 1–20 (2002)	Apr. 2001
968	Riahi, D. N.	Effects of rotation on convection in a porous layer during alloy solidification—Chapter 12 in *Transport Phenomena in Porous Media* (D. B. Ingham and I. Pop, eds.), 316–340 (2002)	Apr. 2001

List of Recent TAM Reports (cont'd)

No.	Authors	Title	Date
969	Damljanovic, V., and R. L. Weaver	Elastic waves in cylindrical waveguides of arbitrary cross section—*Journal of Sound and Vibration* (submitted)	May 2001
970	Gioia, G., and A. M. Cuitiño	Two-phase densification of cohesive granular aggregates—*Physical Review Letters* **88**, 204302 (2002) (in extended form and with added co-authors S. Zheng and T. Uribe)	May 2001
971	Subramanian, S. J., and P. Sofronis	Calculation of a constitutive potential for isostatic powder compaction—*International Journal of Mechanical Sciences* (submitted)	June 2001
972	Sofronis, P., and I. M. Robertson	Atomistic scale experimental observations and micromechanical/continuum models for the effect of hydrogen on the mechanical behavior of metals—*Philosophical Magazine* (submitted)	June 2001
973	Pushkin, D. O., and H. Aref	Self-similarity theory of stationary coagulation—*Physics of Fluids* **14**, 694–703 (2002)	July 2001
974	Lian, L., and N. R. Sottos	Stress effects in ferroelectric thin films—*Journal of the Mechanics and Physics of Solids* (submitted)	Aug. 2001
975	Fried, E., and R. E. Todres	Prediction of disclinations in nematic elastomers—*Proceedings of the National Academy of Sciences* **98**, 14773–14777 (2001)	Aug. 2001
976	Fried, E., and V. A. Korchagin	Striping of nematic elastomers—*International Journal of Solids and Structures* **39**, 3451–3467 (2002)	Aug. 2001
977	Riahi, D. N.	On nonlinear convection in mushy layers: Part I. Oscillatory modes of convection—*Journal of Fluid Mechanics* **467**, 331–359 (2002)	Sept. 2001
978	Sofronis, P., I. M. Robertson, Y. Liang, D. F. Teter, and N. Aravas	Recent advances in the study of hydrogen embrittlement at the University of Illinois—Invited paper, Hydrogen–Corrosion Deformation Interactions (Sept. 16–21, 2001, Jackson Lake Lodge, Wyo.)	Sept. 2001
979	Fried, E., M. E. Gurtin, and K. Hutter	A void-based description of compaction and segregation in flowing granular materials—*Proceedings of the Royal Society of London A* (submitted)	Sept. 2001
980	Adrian, R. J., S. Balachandar, and Z.-C. Liu	Spanwise growth of vortex structure in wall turbulence—*Korean Society of Mechanical Engineers International Journal* **15**, 1741–1749 (2001)	Sept. 2001
981	Adrian, R. J.	Information and the study of turbulence and complex flow—*Japanese Society of Mechanical Engineers Journal B*, in press (2002)	Oct. 2001
982	Adrian, R. J., and Z.-C. Liu	Observation of vortex packets in direct numerical simulation of fully turbulent channel flow—*Journal of Visualization*, in press (2002)	Oct. 2001
983	Fried, E., and R. E. Todres	Disclinated states in nematic elastomers—*Journal of the Mechanics and Physics of Solids* **50**, 2691–2716 (2002)	Oct. 2001
984	Stewart, D. S.	Towards the miniaturization of explosive technology—Proceedings of the 23rd International Conference on Shock Waves (2001)	Oct. 2001
985	Kasimov, A. R., and Stewart, D. S.	Spinning instability of gaseous detonations—*Journal of Fluid Mechanics* (submitted)	Oct. 2001
986	Brown, E. N., N. R. Sottos, and S. R. White	Fracture testing of a self-healing polymer composite—*Experimental Mechanics* (submitted)	Nov. 2001
987	Phillips, W. R. C.	Langmuir circulations—*Surface Waves* (J. C. R. Hunt and S. Sajjadi, eds.), in press (2002)	Nov. 2001
988	Gioia, G., and F. A. Bombardelli	Scaling and similarity in rough channel flows—*Physical Review Letters* **88**, 014501 (2002)	Nov. 2001
989	Riahi, D. N.	On stationary and oscillatory modes of flow instabilities in a rotating porous layer during alloy solidification—*Journal of Porous Media*, in press (2002)	Nov. 2001
990	Okhuysen, B. S., and D. N. Riahi	Effect of Coriolis force on instabilities of liquid and mushy regions during alloy solidification—*Physics of Fluids* (submitted)	Dec. 2001
991	Christensen, K. T., and R. J. Adrian	Measurement of instantaneous Eulerian acceleration fields by particle-image accelerometry: Method and accuracy—*Experimental Fluids* (submitted)	Dec. 2001

List of Recent TAM Reports (cont'd)

No.	*Authors*	*Title*	*Date*
992	Liu, M., and K. J. Hsia	Interfacial cracks between piezoelectric and elastic materials under in-plane electric loading—*Journal of the Mechanics and Physics of Solids*, in press (2002)	Dec. 2001
993	Panat, R. P., S. Zhang, and K. J. Hsia	Bond coat surface rumpling in thermal barrier coatings—*Acta Materialia*, in press (2002)	Jan. 2002
994	Aref, H.	A transformation of the point vortex equations—*Physics of Fluids* **14**, 2395–2401 (2002)	Jan. 2002
995	Saif, M. T. A, S. Zhang, A. Haque, and K. J. Hsia	Effect of native Al_2O_3 on the elastic response of nanoscale aluminum films—*Acta Materialia* **50**, 2779–2786 (2002)	Jan. 2002
996	Fried, E., and M. E. Gurtin	A nonequilibrium theory of epitaxial growth that accounts for surface stress and surface diffusion—*Journal of the Mechanics and Physics of Solids*, in press (2002)	Jan. 2002
997	Aref, H.	The development of chaotic advection—*Physics of Fluids* **14**, 1315–1325 (2002); see also *Virtual Journal of Nanoscale Science and Technology*, 11 March 2002	Jan. 2002
998	Christensen, K. T., and R. J. Adrian	The velocity and acceleration signatures of small-scale vortices in turbulent channel flow—*Journal of Turbulence*, in press (2002)	Jan. 2002
999	Riahi, D. N.	Flow instabilities in a horizontal dendrite layer rotating about an inclined axis—*Proceedings of the Royal Society of London A* (submitted)	Feb. 2002
1000	Kessler, M. R., and S. R. White	Cure kinetics of ring-opening metathesis polymerization of dicyclopentadiene—*Journal of Polymer Science A* **40**, 2373–2383 (2002)	Feb. 2002
1001	Dolbow, J. E., E. Fried, and A. Q. Shen	Point defects in nematic gels: The case for hedgehogs—*Proceedings of the National Academy of Sciences* (submitted)	Feb. 2002
1002	Riahi, D. N.	Nonlinear steady convection in rotating mushy layers—*Journal of Fluid Mechanics* (submitted)	Mar. 2002
1003	Carlson, D. E., E. Fried, and S. Sellers	The totality of soft-states in a neo-classical nematic elastomer—*Proceedings of the Royal Society A* (submitted)	Mar. 2002
1004	Fried, E., and R. E. Todres	Normal-stress differences and the detection of disclinations in nematic elastomers—*Journal of Polymer Science B: Polymer Physics* **40**, 2098–2106 (2002)	June 2002
1005	Fried, E., and B. C. Roy	Gravity-induced segregation of cohesionless granular mixtures—*Lecture Notes in Mechanics*, in press (2002)	July 2002
1006	Tomkins, C. D., and R. J. Adrian	Spanwise structure and scale growth in turbulent boundary layers—*Journal of Fluid Mechanics* (submitted)	Aug. 2002
1007	Riahi, D. N.	On nonlinear convection in mushy layers: Part 2. Mixed oscillatory and stationary modes of convection—*Journal of Fluid Mechanics* (submitted)	Sept. 2002
1008	Aref, H., P. K. Newton, M. A. Stremler, T. Tokieda, and D. L. Vainchtein	Vortex crystals—*Advances in Applied Mathematics* **39**, in press (2002)	Oct. 2002
1009	Bagchi, P., and S. Balachandar	Effect of turbulence on the drag and lift of a particle—*Physics of Fluids* (submitted)	Oct. 2002
1010	Zhang, S., R. Panat, and K. J. Hsia	Influence of surface morphology on the adhesive strength of aluminum/epoxy interfaces—*Journal of Adhesion Science and Technology* (submitted)	Oct. 2002
1011	Carlson, D. E., E. Fried, and D. A. Tortorelli	On internal constraints in continuum mechanics—*Journal of Elasticity* (submitted)	Oct. 2002
1012	Boyland, P. L., M. A. Stremler, and H. Aref	Topological fluid mechanics of point vortex motions—*Physica D*, in press (2002)	Oct. 2002